European Journal of Medicinal Chemistry 182 (2019) 111607

Contents lists available at ScienceDirect

European Journal of Medicinal Chemistry

journal homepage: http://www.elsevier.com/locate/ejmech

Research paper

1,2,4-Oxadiazole derivatives targeting EGFR and c-Met degradation in TKI resistant NSCLC

Eman M.E. Dokla [a, 1], Chun-Sheng Fang [b, 1], Khaled A.M. Abouzid [a, c, **], Ching S. Chen [b, d, *]

[a] Pharmaceutical Chemistry Department, Faculty of Pharmacy, Ain Shams University, Abbassia, Cairo, 11566, Egypt
[b] Institute of New Drug Development, China Medical University, Taichung, 40402, Taiwan
[c] Department of Organic and Medicinal Chemistry, Faculty of Pharmacy, University of Sadat City, Menoufia, Egypt
[d] Department of Medical Research, China Medical University Hospital, China Medical University, Taichung, 40447, Taiwan

ARTICLE INFO

Article history:
Received 22 July 2019
Received in revised form
2 August 2019
Accepted 7 August 2019
Available online 9 August 2019

Keywords:
1,2,4-Oxadiazoles
Oncoprotein degradation
EGFR
c-Met
TKI resistant NSCLC

ABSTRACT

Development of small-molecule agents with the ability to facilitate oncoprotein degradation has emerged as a promising strategy for cancer therapy. Since EGFR and c-Met are both implicated in oncogenesis and tumor progression, we initiated a screening program by using an in-house library to identify agents capable of inducing the concomitant suppression of EGFR and c-Met expression, which led to the identification of compound **1**, a 1,2,4-oxadiazole derivative. Based on the scaffold of **1**, we developed a series of derivatives to assess their efficacies in facilitating the downregulation of EGFR and c-Met, among which compound **48** represented the optimal agent. **48** showed equipotent antiproliferative activity against a panel of five NSCLC cell lines with different EGFR mutational status ($IC_{50} = 0.2-0.6\ \mu M$), while the same panel exhibited differential sensitivity to different EGFR kinase inhibitors tested. Cell cycle analysis indicated that the antiproliferative activity of **48** was associated with its ability to cause G2/M arrest and, to a lesser extent, apoptosis. Western blot and RT-PCR analyses revealed that **48** facilitated the downregulation of EGFR and c-Met at the protein level. *In vivo* data showed that oral administration of **48** was effective in suppressing gefitinib-resistant H1975 xenograft tumor growth in nude mice, and at a suboptimal dose, could sensitize H1975 tumors to gefitinib. Based on these findings, **48** represents a promising candidate for further development to target EGFR TKI-resistant NSCLC via dual inhibition of EGFR and c-Met oncoproteins.

1. Introduction

Despite extensive efforts directed toward developing effective therapies to fight cancer in the past two decades, it remains a threatening challenge worldwide. While conventional cancer therapies are non-discriminative between normal and malignant cells, targeted therapy acts by blocking essential biochemical pathways or oncoproteins that are required for tumor cell growth and survival, thereby selectively killing cancer cells over normal cells [1]. Although targeting oncogenic proteins inhibition represents a valuable approach to tackle cancer [2], such approach was limited by the number of undruggable targets and the development of resistance. A more effective strategy was soon developed to overcome these limitations by targeting oncoproteins degradation rather than merely inhibiting them [3,4]. This strategy involves the use of small interfering RNA that acts on the gene expression level or the use of chemical inducers that acts on post-translational level [5,6].

Epidermal Growth Factor Receptor (EGFR) belongs to the ErbB family of receptor tyrosine kinases [7] and it is over-expressed in lung, colon and breast cancers [8]. On the other hand c-Met, another receptor tyrosine kinase, can result in tumor growth and progression in gastric, esophageal, colon and lung cancers [9]. Several small molecule tyrosine kinase inhibitors (TKIs) were developed to inhibit both kinases, but due to the development of resistance (e.g. EGFR mutation, c-Met over-expression), many of these agents were rendered ineffective or of limited clinical use [10]. Several approaches were proposed to target EGFR-TKI

* Corresponding author. Institute of New Drug Development, China Medical University, Taichung, 40402, Taiwan.
** Corresponding author. Pharmaceutical Chemistry Department, Faculty of Pharmacy, Ain Shams University, Abbassia, Cairo, 11566, Egypt.
E-mail addresses: khaled.abouzid@pharma.asu.edu.eg (K.A.M. Abouzid), cschencmu@gmail.com (C.S. Chen).
[1] Both authors have equal contributions.

https://doi.org/10.1016/j.ejmech.2019.111607
0223-5234/

resistant cancers [11], including design of new irreversible TKIs [12,13], use of anti-EGFR antibodies [14,15], development of TKI-combinations [16,17], or targeting EGFR and other related oncoproteins degradation [18].

Several Hsp90 inhibitors (Fig. 1) were reported to target TKI resistant cancer cell lines via promoting the degradation of several kinases including EGFR and c-Met. A chalcone derivative **1f** was reported to inhibit Hsp90 with subsequent degradation of EGFR, c-Met, Her2 and Akt kinases. **1f** showed modest antiproliferative activity against gefitinib-resistant NSCLC cell line (H1975) ($GI_{50} = 48$ mM) [19]. **STA-9090** is another Hsp90 inhibitors developed by Synta pharmaceuticals. It is a triazole derivative (structure not disclosed) that exhibited potent activity against several TKI resistant human cancer cell lines at nanomolar concentrations via inducing the degradation of several oncogenic proteins including mutated EGFR and c-Met [20]. A thiochromeno[2,3-c]quinolin-12-one derivative, **TC-N19**, was reported to target the degradation of EGFR and c-Met in resistant NSCLC [21,22]. Recently an Hsp90 inhibitor; **DPide** was reported to exert a potent antiproliferative activity against triple-negative breast cancer and NSCLC cell lines (MDA-MB-231 and H1975 with a GI_{50} of 0.478 and 1.67 μM respectively). Such activity is postulated to be mediated through proteasomal degradation of EGFR, Her2, Met, Akt, c-Raf, and Cdk4 [23]. **T315** is a pyrazole-based small molecule (Fig. 1) first reported as an integrin-linked kinase (ILK) inhibitor [24]. In a subsequent study, this compound was reported to inhibit EGFR-TKI resistant lung adenocarcinoma via promoting EGFR degradation through the ubiquitin-proteasome pathway [25]. These small molecules represent a proof of concept that targeting EGFR and c-Met oncoprotein degradation can provide an alternative pathway to treat TKI resistant cancers.

Till today, screening chemical libraries still provides an important resource for identification of valuable lead compounds especially for new biological targets [26]. As targeting oncoprotein degradation represents an attractive strategy for anti-cancer drug discovery, we initiated a screening of our in-house compound libraries to identify agents capable of facilitating the degradation of EGFR by using MDA-MB-231 breast cancer cells as a cell model. This screening program led to the identification of an oxadiazole derivative, **1** [*N*-(4-(5-(3-benzamidophenyl)-1,2,4-oxadiazol-3-yl)-3-chlorophenyl)-nicotinamide] (Fig. 2), which exhibited a unique, yet modest ability to concomitantly down-regulate the expression of EGFR and another oncogenic receptor tyrosine kinase, c-Met (Fig. 3). In this study, we developed a series of dual-target inhibitors, represented by compound **48**, which exhibited high efficacy in inducing the degradation of EGFR and c-Met oncoproteins.

2. Results and discussion

2.1. Chemistry

The synthesis of the desired 1,2,4-oxadiazole derivatives **1**–**50** was achieved through the synthetic route outlined in Scheme 1. Stirring nicotinoyl chloride hydrochloride (**I**) and the appropriate 4-aminobenzonitrile (**IIa-g**) in acetonitrile and triethylamine at room temperature furnished benzonitrile intermediates (**IIIa-g**) in 50–90% yield. Heating **IIIa-g** with hydroxylamine solution in ethanol gave the amidoxime intermediates (**IVa-g**) in 80–100% yield. Cyclization of **IVa-g** was achieved by reacting with 3-nitrobenzoyl chloride in pyridine at 100 °C to give the 1,2,4-oxadiazole intermediates (**Va-g**) in 60–95% yield. Reduction of **Va-g** was achieved using $SnCl_2 \cdot 2H_2O$ in EtOAc under refluxing conditions to give the amino intermediates (**VIa-g**) in 40–80% yield. Compound **1** was prepared in 64% yield by acylating the amine derivative (**VIc**) with benzoyl chloride in pyridine. Compounds **2**–**24** were synthesized by reacting the amine derivative (**VIa-g**) with the respective sulfonyl chloride in pyridine at room temperature to furnish the desired final compounds **2**–**24** in 20–81% yield. Compounds **25**–**50** were prepared in two steps by heating the amine derivatives (**VIc**) with phosgene in dry THF to give the corresponding isocyanate intermediates, which was used immediately, without purification, to react with appropriate aniline derivatives and *N*,*N*-diisopropylethylamine (DIPEA) in dry THF to afford the desired final compounds **25**–**50** in 15–90% yield.

2.2. Biological activities

2.2.1. In vitro antiproliferative screening in MDA-MB-231 cells

In light of the modest potency of **1** in suppressing EGFR and c-Met expression in MDA-MB-231 cells (cell viability IC_{50}, 12.8 μM after 72 h; MTT assays), we conducted several optimization cycles based on the modifications of ring A, ring B, and linker C, which generated four series of derivatives consisting of a total of 49 compounds (Fig. 2), according to a synthetic scheme depicted in Scheme 1. The antiproliferative activities of these compounds were first evaluated in MDA-MB-231 cells (Fig. 2) by MTT assays to help identify optimal agents. In series I, bioisosteric replacement of the amide linker C with a sulfonamide, followed by adding various substituents at position 3 and/or 4 on ring A gave inactive compounds except for compound **8** (IC_{50}, 2.5 μM). Subsequent optimization of **8** included the replacement of the 2-Cl moiety on ring B with various substituents at position 2 or 3 and the acetamido moiety on ring A with different urea functions, generating series II (**11**–**16**) and III (**17**–**24**), respectively. Except for compound **18** (IC_{50}, 1.3 μM), these modifications did not yield derivatives with improved potency. Furthermore, replacement of the amide linker C with a urea, followed by substitutions on ring A with various functional groups at position 3 and/or 4 generated an array of derivatives (series IV, **25**–**50**) with a broad range of anti-proliferative activity, especially noteworthy were those with IC_{50} values < 1 μM in our initial screening, including **39**–**43**, **47** and **48**.

2.2.2. Western blot analysis in MDA-MB-231 cells

As part of the mechanistic validation, seven representative

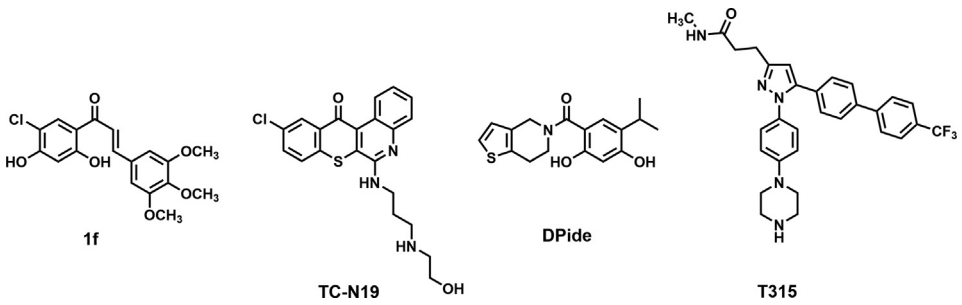

Fig. 1. Chemical structures of reported small molecules targeting EGFR and c-Met Degradation via different mechanisms.

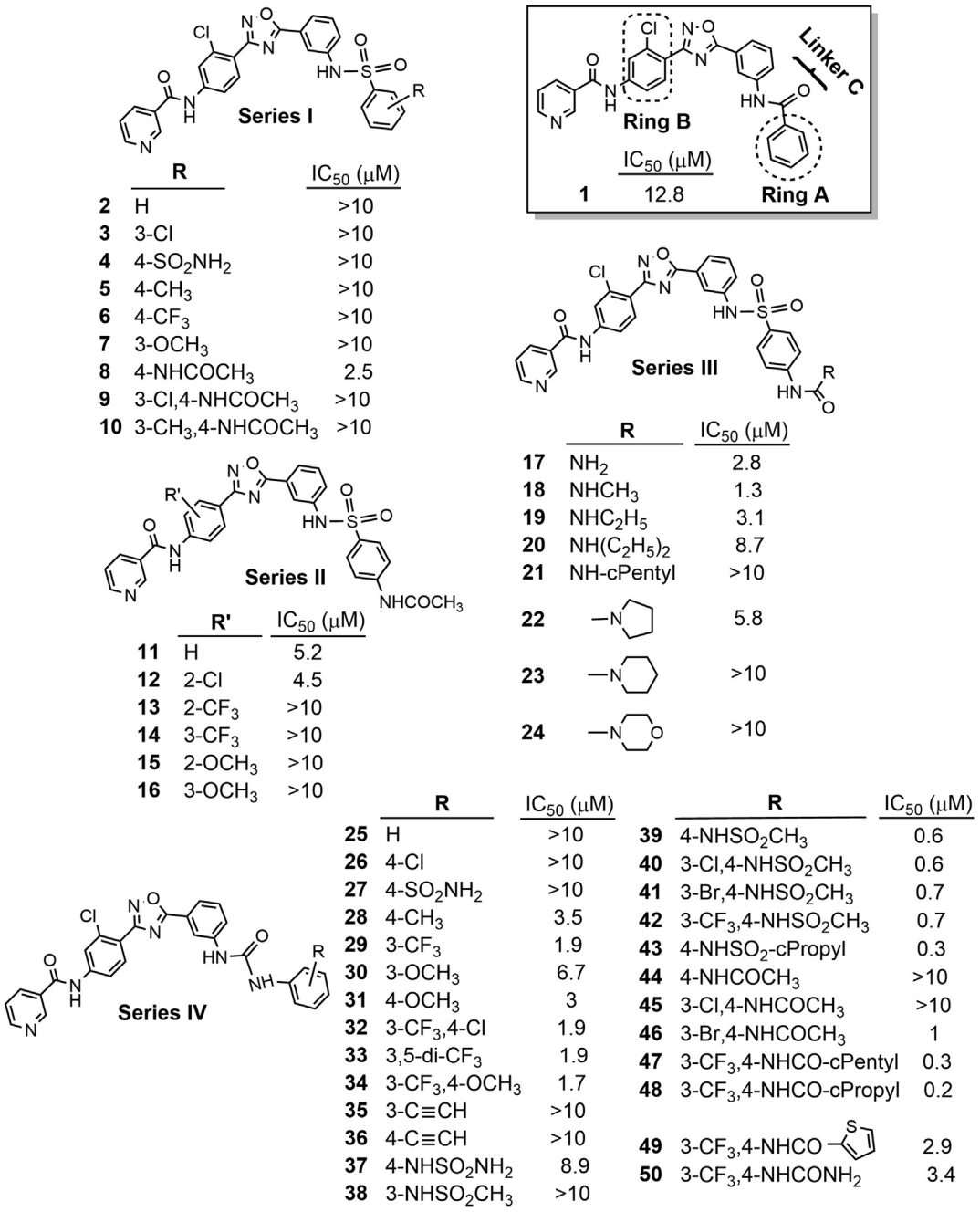

	R	IC_{50} (μM)
1		12.8
2	H	>10
3	3-Cl	>10
4	4-SO_2NH_2	>10
5	4-CH_3	>10
6	4-CF_3	>10
7	3-OCH_3	>10
8	4-$NHCOCH_3$	2.5
9	3-Cl,4-$NHCOCH_3$	>10
10	3-CH_3,4-$NHCOCH_3$	>10

	R'	IC_{50} (μM)
11	H	5.2
12	2-Cl	4.5
13	2-CF_3	>10
14	3-CF_3	>10
15	2-OCH_3	>10
16	3-OCH_3	>10

	R	IC_{50} (μM)
17	NH_2	2.8
18	$NHCH_3$	1.3
19	NHC_2H_5	3.1
20	$NH(C_2H_5)_2$	8.7
21	NH-cPentyl	>10
22		5.8
23		>10
24		>10

	R	IC_{50} (μM)
25	H	>10
26	4-Cl	>10
27	4-SO_2NH_2	>10
28	4-CH_3	3.5
29	3-CF_3	1.9
30	3-OCH_3	6.7
31	4-OCH_3	3
32	3-CF_3,4-Cl	1.9
33	3,5-di-CF_3	1.9
34	3-CF_3,4-OCH_3	1.7
35	3-C≡CH	>10
36	4-C≡CH	>10
37	4-$NHSO_2NH_2$	8.9
38	3-$NHSO_2CH_3$	>10

	R	IC_{50} (μM)
39	4-$NHSO_2CH_3$	0.6
40	3-Cl,4-$NHSO_2CH_3$	0.6
41	3-Br,4-$NHSO_2CH_3$	0.7
42	3-CF_3,4-$NHSO_2CH_3$	0.7
43	4-$NHSO_2$-cPropyl	0.3
44	4-$NHCOCH_3$	>10
45	3-Cl,4-$NHCOCH_3$	>10
46	3-Br,4-$NHCOCH_3$	1
47	3-CF_3,4-NHCO-cPentyl	0.3
48	3-CF_3,4-NHCO-cPropyl	0.2
49	3-CF_3,4-NHCO-	2.9
50	3-CF_3,4-$NHCONH_2$	3.4

Fig. 2. Structures of 1,2,4-oxadiazole-based compounds **1**–**50** and their respective antiproliferative IC_{50} values measured in MDA-MB-231 cells by MTT assays after 72 h of drug treatment.

oxadiazole derivatives with varying antiproliferative potencies (**29**, **34**, **39**, **40**, **43**, **47**, and **48**) vis-à-vis compound **1** were tested for their abilities to suppress the expression of EGFR and c-Met in MDA-MB-231 cells. As shown in Fig. 3, among these seven derivatives, only compounds **43**, **47**, and **48** exhibited a suppressive effect on the expression of both oncoproteins with potencies parallel to the respective anti-proliferative activities. Although compounds **29**, **34**, **39**, and **40** were able to inhibit the expression of c-Met, their suppressive effect on EGFR was less evident. As EGFR and c-Met represent important therapeutic targets for lung cancer, we used lung cancer cell lines with different EGFR mutational status to elucidate the mode of antitumor mechanism of the optimal agent **48**.

2.2.3. In vitro antiproliferative efficacy of compound 48 in a panel of NSCLC cell lines with different EGFR mutational status

In this study, we used five NSCLC cell lines with different EGFR mutational status to interrogate the effect of **48** on EGFR and c-Met expression, including A549 (wild type), PC9 (DelE746-A750 [27]), H1975 (L858R [27] + T790M [28]), CL68 (DelE746-A750 + T790M), and CL97 (G719A [29] + T790M). These NSCLC cell lines was first characterized by their susceptibilities to four different TKIs by MTT assays, including the first-generation TKIs gefitinib and erlotinib and the irreversible TKIs afatinib and omisertinib. While PC9 cells were extremely sensitive to all four TKIs, (IC_{50} values at 72 h: $\leq$ 0.1 μM), the other cell lines examined (A549, H1975, CL68, and CL97) were resistant to gefitinib and erlotinib (IC_{50} values at 72 h:

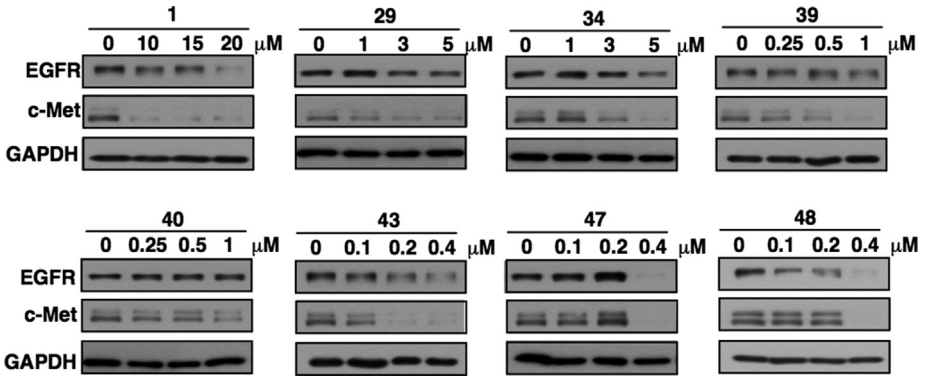

Fig. 3. Western blot analysis of the effect of compound **1** and its derivatives, at indicated concentrations, on the expression of EGFR and c-Met in MDA-MB-231 cells after 48 h of drug treatment.

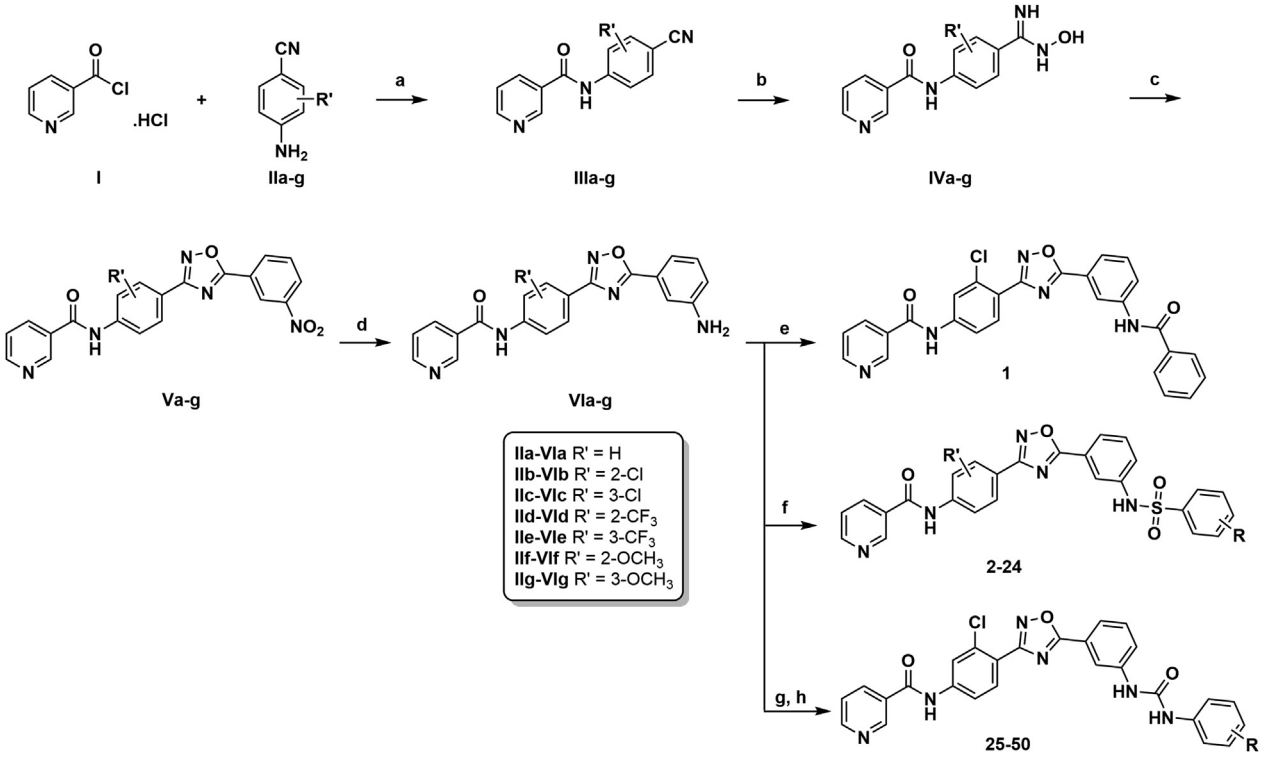

Scheme 1. Synthesis of oxadiazole derivatives 1–50. Reagents and Conditions. (a) CH_3CN, TEA, rt, overnight; (b) NH_2OH (50% in water), EtOH, reflux, 24 h; (c) 3-Nitrobenzoyl chloride, pyridine, 100 °C, 16 h; (d) $SnCl_2 \cdot 2H_2O$, EtOAc, reflux, 24 h; (e) Benzoyl chloride, THF, pyridine, rt, 4 h; (f) $ArSO_2Cl$, pyridine, rt, 24 h; (g) Phosgene, THF, reflux, 4 h; (h) $ArNH_2$, THF, DIPEA, reflux, overnight.

5–20 μM) (Table 1). In contrast, **48** exhibited consistent antiproliferative potency among these five cell lines, with IC_{50} values ranging from 0.3 to 0.6 μM and 0.2–0.5 μM after 48 and 72 h of treatment respectively (Table 1 and Fig. 4A).

2.2.4. Western blot, RT-PCR and flow cytometric analyses of the effect of compound 48 on a panel of NSCLC cell lines

Western blot analysis confirmed the ability of **48**, in the range of 0.2–0.6 μM after 48 h treatment, to suppress the expression of EGFR and c-Met in these five cell lines irrespective of their mutational status (Fig. 4B), which correlates with its ability to inhibit the proliferation of these NSCLC cell lines. Apart from CL68 cells, this downregulation of EGFR expression was accompanied by a parallel decrease in Akt phosphorylation, suggesting differences in the regulation of EGFR-mediated Akt activation in CL68 cells. Moreover, RT-PCR analysis showed that the mRNA levels of EGFR and c-Met remained unaltered in response to **48** at 0.2–0.6 μM in H1975 and A549 cells (Fig. 4C), indicating that the drug effect was mediated at the protein level. Cell cycle analysis using propidium iodide showed that the antiproliferative effect of **48** was mainly associated with G2/M arrest and, to a lesser extent, apoptosis (Fig. 4D), which is consistent with a reported finding that siRNA-mediated knockdown of EGFR caused G2/M arrest in cancer cells [30].

2.2.5. In vivo efficacy of compound 48 in nude mice H1975 xenograft tumor model

Pursuant to the above findings, we tested the *in vivo* tumor-suppressive efficacy of compound **48** in athymic nude mice bearing subcutaneous H1975 xenograft tumors. H1975 cells are resistant to the first-generation EGFR-TKIs (Table 1) because these

Table 1
The antiproliferative efficacies (IC_{50} in μM) of four TKIs in comparison to compound 48 on five lung adenocarcinoma cell lines determined by MTT assays after 48–72 h treatment.

Cell lines	EGFR mutation	Gefitinib (1st gen. TKI)	Erlotinib (1st gen. TKI)	Afatinib (2nd gen. TKI)	Omisertinib (3rd gen. TKI)	Compound 48	
		72 h (μM)				48 h (μM)	72 h (μM)
A549	WT[a]	20	20	5–10	5	0.3	0.2
PC9	delE746-A750[b]	0.1	0.1	<0.01	<0.01	0.6	0.5
H1975	L858R[c] + T790M[d]	10–20	10	1	0.05	0.3	0.3
CL68	delE746-A750 + T790M	5	5	0.1	0.01	0.5	0.4
CL97	G719A[e] + T790M	10–20	>20	0.1	0.1	0.6	0.5

[a] WT: wild-type.
[b] delE746-A750: 747 to 750 frame deletion of amino acids in exon 19 [27].
[c] L858R: single-point mutation of leucine to arginine at codon 858 in exon 21 [27].
[d] T790M: threonine to methionine mutation at position 790 in exon 20 [28].
[e] G719A: single-point mutation of glycine to alanine at codon 719 in exon 18 [29].

cells harbor the gatekeeper mutation T790M [31–33]. As shown, daily oral administration of **48**, at 50 or 150 mg/kg, versus vehicle via gavage (n = 8 for each group) exhibited a dose-dependent suppression (29% and 60%, respectively) of H1975 xenograft tumor growth relative to vehicle control at the end of the 20 day-treatment (Fig. 5A, left panel; $^{*}P < 0.05$). **48** was well tolerated by tumor-bearing mice as no appreciable weight loss was noted in both drug-treated groups, indicating that no acute toxicities were associated with drug treatment (Fig. 5A, right panel). Western blot analysis of tumor lysates showed that this tumor-suppressive activity correlated with the ability of **48** to inhibit the expression of EGFR and c-Met in a dose-dependent manner (Fig. 5B). In light of the cross-activation between EGFR and c-Met in lung cancer cells, dual targeting of EGFR and c-Met has been reported to be an effective strategy against T790M EGFR-mediated TKI resistant lung cancer [17]. Consequently, we assessed the ability of **48** at a suboptimal dose to sensitize H1975 xenograft tumors to gefitinib. As shown, combination of **48** and gefitinib, each at 50 mg/kg daily via oral gavage, gave rise to a higher extent of tumor suppression (72%) relative to individual drugs alone (Fig. 5C; **48**, 37%; gefitinib, 27%).

3. Conclusion

In this study we report the identification of a 1,2,4-oxadiazole-based small molecule, compound **48**, that exhibited a unique ability to co-target EGFR and c-Met oncoprotein degradation. **48** showed potent antiproliferative activity against MDA-MB-231 and a panel of NSCLC cell lines. While the activities of four TKIs used for comparison were variable conforming to the type of EGFR mutation, the efficacy of **48** was consistent irrespective of EGFR mutational status. Moreover, **48** showed a dose-dependent tumor-suppressive activity in TKI resistant H1975 xenograft tumors and was effective in sensitizing these tumors to gefitinib at a suboptimal dose. Accordingly, **48** provides a proof-of-concept that concomitant targeting EGFR and c-Met degradation, in lieu of dual kinase activity inhibition, might represent an alternative strategy to circumvent EGFR mutation-mediated resistance, which is associated with even the 3rd-generation irreversible TKIs [34]. Further optimization and mechanistic validation of the exact molecular target of **48** will help establish this series as a preclinical candidate to treat EGFR-TKI resistant tumors.

4. Experimental

4.1. Chemistry

Detailed information on the syntheses and pertinent spectroscopic data of the intermediates and final compounds **1** to **50** is described in the **Supplementary data**. All commercially available reagents were used without further purification unless otherwise stated. Routine ^{1}H and ^{13}C nuclear magnetic resonance spectra were recorded on Bruker AV300 or Bruker Ascend 400. Samples were dissolved in deuterated chloroform ($CDCl_3$) or dimethyl sulfoxide (DMSO-d_6), and tetramethylsilane (TMS) was used as a reference. Electrospray ionization mass spectrometry analyses were performed with a Micromass Q-T of II high resolution electrospray mass spectrometer at The Ohio State University Campus Chemical Instrument Center. All compounds for bioassay were identified with ^{1}H NMR, ^{13}C NMR, and HRMS, and in purity higher than 95%. The purity of was confirmed by a Hitachi Elite LaChrom HPLC system (comprised of a Versa Grad Prep 36 pump, an L-2400 UV detector, an L-2200 auto sampler and a 150 × 4.6 mm Agilent ZORBAX Eclipse XDB-C18 5μ column; detection, 254 nm). A linear solvent gradient with a mobile phase of 30% water in methanol to 100% methanol in 20 min was used.

4.1.1. General synthetic procedures for compounds 1-50

Step a: To an ice-cold suspension of nicotinoyl chloride hydrochloride (**I**) (1.78 g, 10 mmol) and appropriate 4-aminobenzonitrile (**IIa-g**) (10 mmol, 1.0 equiv) in acetonitrile (50 ml) under nitrogen was added triethylamine (8.1 g, 11.15 ml, 40 mmol, 4.0 equiv) dropwise over 30 min. The resulting suspension was stirred at 0 °C for 1 h then at room temperature overnight. The reaction mixture was evaporated, diluted with EtOAc, washed with 10% HCl, brine, dried over anhydrous Na_2SO_4 and concentrated in vacuo. The resulting solid was washed with diethyl ether and dried to yield the desired compounds (**IIIa-g**) in 50–90% yield.
Step b: To a solution of appropriate benzonitrile (**IIIa-g**) (10 mmol, 1 equiv) in ethanol (100 ml) was added hydroxylamine solution (50% in water, 2 ml, 30 mmol, 3.0 equiv) and the reaction mixture was refluxed for 24 h. The reaction mixture was evaporated, then dried under vacuum to give the desired amidoxime derivatives (**IVa-g**) in 80–100% yield.
Step c: To a solution of appropriate amidoxime (**IVa-g**) (10 mmol, 1.0 equiv) in pyridine (50 ml) was added 3-nitrobenzoyl chloride (2.78 g, 15 mmol, 1.5 equiv) portion wise with stirring. The reaction mixture was heated at 100 °C for 16 h. The solution was cooled and added to ice/water (500 ml) with vigorous stirring, then kept in refrigerator overnight. The precipitated solid was filtered, washed with water, diethyl ether and dried in vacuo to give the desired 1,2,4-oxadiazole derivatives (**Va-g**) in 60–95% yield.

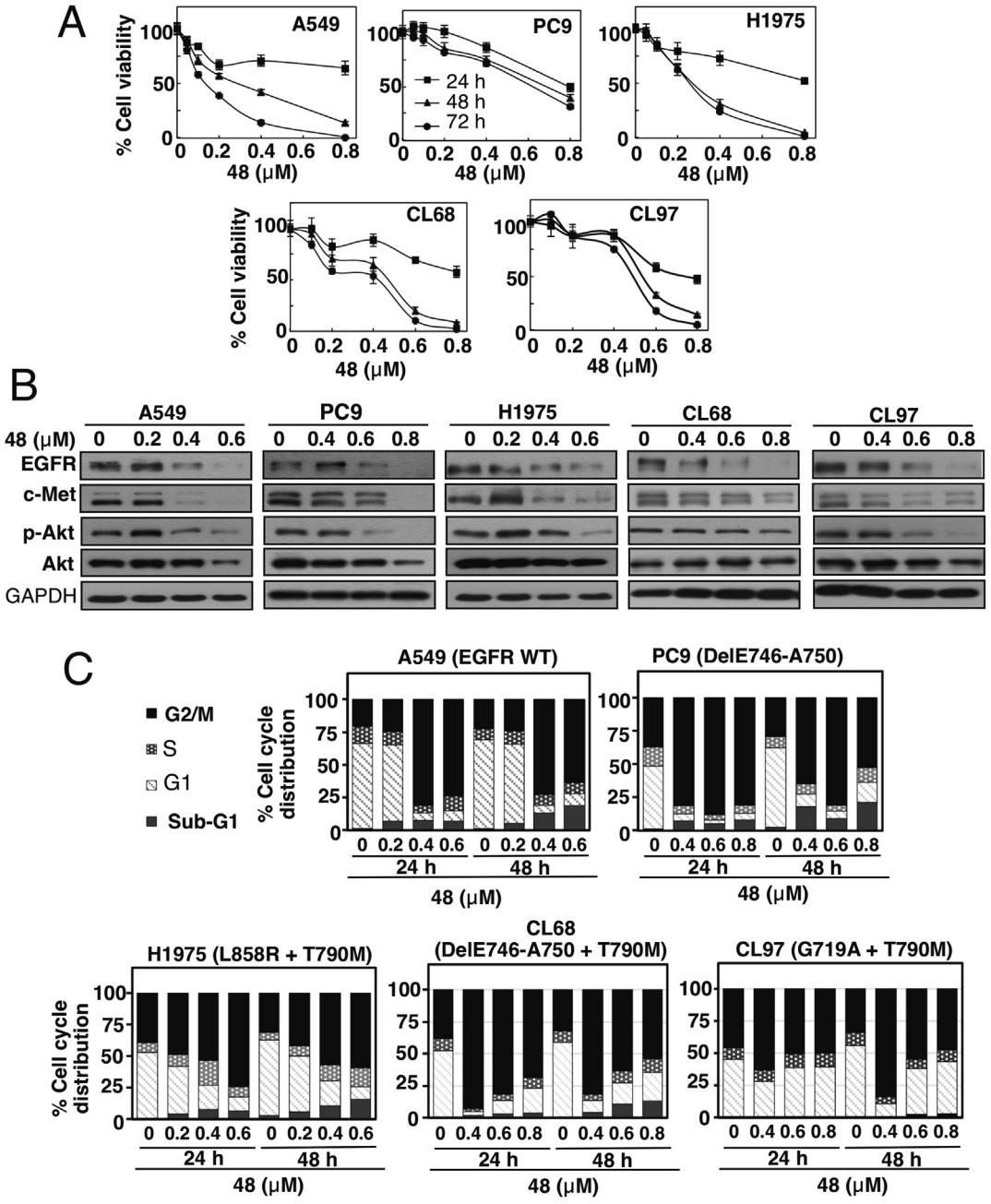

Fig. 4. (**A**) MTT assays of the time- and dose-dependent inhibitory effect of **48** on the viability of A549, PC9, H1975, CL68, and CL97 cells at different time intervals (■, 24 h; ▲, 48 h; •, 72 h). Data are presented as means ± S.D (n = 6). (**B**) Western blot analysis of the dose-dependent effects of **48** on the expression/phosphorylation of EGFR, c-Met, and Akt after 48 h treatment. (**C**) RT-PCR analysis of the effect of **48** on EGFR and c-Met mRNA expression in H1975 and A549 cells. (**D**) Flow cytometric analysis of the dose-dependent effects of **48** on the cell cycle distribution after 24 and 48 h of treatment.

Step d: To a suspension of the appropriate nitro derivative (**Va-g**) (5 mmol, 1.0 equiv) in EtOAc (100 ml) was added $SnCl_2 \cdot 2H_2O$ (5.6 g, 25 mmol, 5.0 equiv) and the reaction mixture was refluxed for 24 h. Upon completion of the reaction as indicated by TLC, the mixture was cooled, washed with 1N NaOH, brine, dried over anh. Na_2SO_4, filtered and concentrated in vacuo to give the desired amino compounds (**VIa-g**) in 40–80% yield.

Step e: To an ice cold solution of *N*-[4-[5-(3-aminophenyl)-1,2,4-oxadiazol-3-yl]-3-chlorophenyl]-3-pyridinecarboxamide (**VIc**) (0.1 g, 0.26 mmol, 1 equiv) in THF (10 ml) and pyridine (0.04 g, 41 μl, 0.52 mmol, 2 equiv) was added benzoyl chloride (0.053 g, 44 μl, 0.38 mmol, 1.5 equiv) and the reaction mixture was stirred at room temperature for 4 h. Upon completion of the reaction as indicated by TLC, the solution was concentrated and the residue was purified by chromatography to give the desired final products **1.**

*4.1.1.1. N-[3-chloro-4-[5-[3-[(benzoyl)amino]phenyl]-1,2,4-oxadiazol-3-yl]phenyl]-3-pyridinecarboxamide (**1**).* $R_f = 0.25$ (DCM/MeOH 9:1). White solid, yield 64%. ^{1}H NMR (300 MHz, DMSO-d_6) δ 10.88 (s, 1H), 10.62 (s, 1H), 9.14 (dd, *J* = 2.3, 0.9 Hz, 1H), 8.85–8.71 (m, 2H), 8.33 (dt, *J* = 7.9, 2.0 Hz, 1H), 8.27–7.88 (m, 7H), 7.72–7.50 (m, 5H).

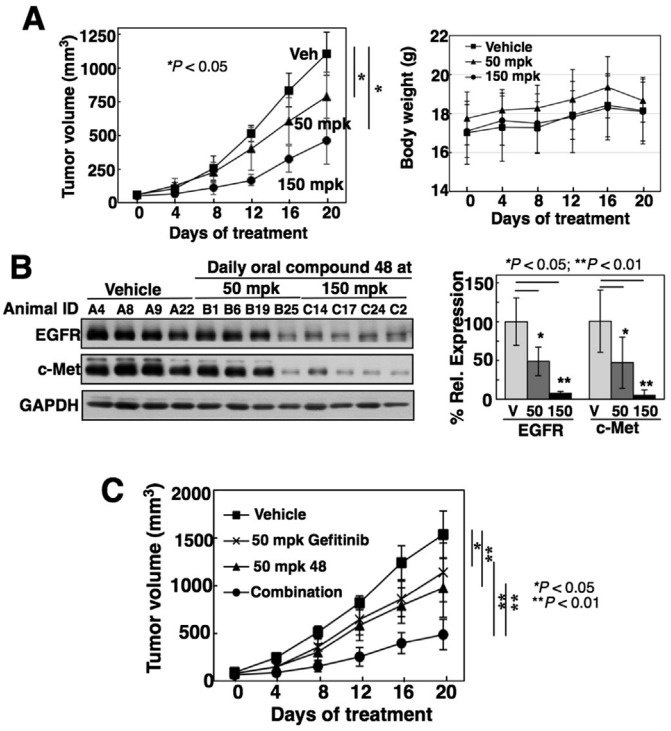

Fig. 5. ***In vivo*** **efficacy of compound 48, alone or in combination with gefitinib, in suppressing H1975 xenograft tumors.** (**A**) Effect of **48** at 50 and 150 mg/kg daily (mpk) versus vehicle control, via oral gavage, on tumor volume (left) and body weight (right) in H1975 xenograft model (n = 8/each group) throughout a 20-day treatment period. Points, means ± S.E. (n = 8). (**B**) Immunoblotting analysis (left) of EGFR and c-Met in tumor lysates of four representative tumors from each group and analysis of relative expression values (right) of individual markers based on densitometric quantitation of band intensities. (**C**) Effect of the combination of **48** and gefitinib versus single agents, each at 50 mg/kg daily via oral gavage, on tumor volume in H1975 xenograft model (n = 7/each group) after 20 days of treatment. The data are presented as means ± S.E. (*P < 0.05, **P < 0.01).

Step f: To a cooled solution of the appropriate *N*-[4-[5-(3-aminophenyl)-1,2,4-oxadiazol-3-yl]substituted phenyl]-3-pyridinecarboxamide (**VIa-g**) (0.26 mmol, 1 equiv) in pyridine (10 ml) was added the appropriate sulfonyl chloride derivative (0.38 mmol, 1.5 equiv) and the reaction mixture was stirred at room temperature overnight. Upon completion of the reaction as indicated by TLC, the solution was concentrated, stirred with cold water and the resulting precipitate was filtered, dried and purified by chromatography to give the desired final products (**2**–**24**).

*4.1.1.2. N-[3-chloro-4-[5-[3-[(phenylsulfonyl)amino]phenyl]-1,2,4-oxadiazol-3-yl] phenyl]-3-pyridinecarboxamide (**2**).* $R_f = 0.30$ (EtOAc/Hexane 3:1). White solid, yield 65%. ^{1}H NMR (300 MHz, DMSO-d_6) δ 10.84 (s, 1H), 10.74 (s, 1H), 9.15 (d, $J = 1.9$ Hz, 1H), 8.80 (dd, $J = 4.8$, 1.5 Hz, 1H), 8.33 (dt, $J = 7.9$, 1.9 Hz, 1H), 8.21 (d, $J = 1.9$ Hz, 1H), 8.04 (d, $J = 8.6$ Hz, 1H), 7.99–7.90 (m, 2H), 7.87–7.80 (m, 3H), 7.69–7.49 (m, 5H), 7.49–7.38 (m, 1H).

*4.1.1.3. N-[3-chloro-4-[5-[3-[(3-chlorophenylsulfonyl)amino]phenyl]-1,2,4-oxadiazol-3-yl]phenyl]-3-pyridinecarboxamide (**3**).* $R_f = 0.30$ (EtOAc/Hexane/MeOH 4:4:0.25). White solid, yield 68%. ^{1}H NMR (300 MHz, DMSO-d_6) δ 10.87 (s, 2H), 9.14 (dd, $J = 2.4$, 0.9 Hz, 1H), 8.80 (dd, $J = 4.8$, 1.6 Hz, 1H), 8.33 (dt, $J = 8.0$, 2.0 Hz, 1H), 8.22 (d, $J = 2.0$ Hz, 1H), 8.05 (d, $J = 8.6$ Hz, 1H), 7.99–7.82 (m, 4H), 7.79–7.69 (m, 2H), 7.67–7.52 (m, 3H), 7.46 (dt, $J = 8.6$, 1.3 Hz, 1H).

*4.1.1.4. N-[4-[5-[3-[[4-(aminosulfonyl)phenylsulfonyl]amino] phenyl]-1,2,4-oxadiazol-3-yl]3-chlorophenyl]-3-pyridinecarboxamide (**4**).* $R_f = 0.25$ (EtOAc/Hexane/MeOH 4:2:0.25). White solid, yield 69%. ^{1}H NMR (300 MHz, DMSO-d_6) δ 10.98 (s, 1H), 10.87 (s, 1H), 9.14 (d, $J = 1.4$ Hz, 1H), 8.80 (dd, $J = 4.8$, 1.6 Hz, 1H), 8.33 (dt, $J = 8.0$, 2.0 Hz, 1H), 8.22 (d, $J = 2.0$ Hz, 1H), 8.17–7.93 (m, 7H), 7.88 (dt, $J = 7.9$, 1.3 Hz, 1H), 7.66–7.52 (m, 4H), 7.49–7.42 (m, 1H).

*4.1.1.5. N-[3-chloro-4-[5-[3-[(4-methylphenylsulfonyl)amino] phenyl]-1,2,4-oxadiazol-3-yl]phenyl]-3-pyridinecarboxamide (**5**).* $R_f = 0.20$ (EtOAc/Hexane/MeOH 4:4:0.25). White solid, yield 45%. ^{1}H NMR (300 MHz, DMSO-d_6) δ 10.84 (s, 1H), 10.66 (s, 1H), 9.15 (dd, $J = 2.4$, 0.8 Hz, 1H), 8.80 (dd, $J = 4.8$, 1.6 Hz, 1H), 8.33 (dt, $J = 8.0$, 2.0 Hz, 1H), 8.22 (d, $J = 2.0$ Hz, 1H), 8.04 (d, $J = 8.6$ Hz, 1H), 7.99–7.92 (m, 2H), 7.83 (dt, $J = 7.8$, 1.3 Hz, 1H), 7.71 (d, $J = 8.3$ Hz, 2H), 7.65–7.49 (m, 2H), 7.49–7.41 (m, 1H), 7.37 (d, $J = 8.1$ Hz, 2H), 2.33 (s, 3H).

*4.1.1.6. N-[3-chloro-4-[5-[3-[[4-(trifluoromethyl)phenylsulfonyl] amino]phenyl]-1,2,4-oxadiazol-3-yl]phenyl]-3-pyridinecarboxamide (**6**).* $R_f = 0.35$ (EtOAc/Hexane/MeOH 4:4:0.25). White solid, yield 63%. ^{1}H NMR (400 MHz, DMSO-d_6) δ 10.88–10.82 (m, 2H), 9.14 (d, $J = 2.2$ Hz, 1H), 8.80 (dd, $J = 4.8$, 1.6 Hz, 1H), 8.33 (dt, $J = 8.0$, 2.1 Hz, 1H), 8.21 (d, $J = 2.1$ Hz, 1H), 8.05–8.00 (m, 2H), 8.00–7.73 (m, 5H), 7.66–7.40 (m, 3H), 7.08 (d, $J = 8.9$ Hz, 1H).

*4.1.1.7. N-[3-chloro-4-[5-[3-[(3-methoxyphenylsulfonyl)amino] phenyl]-1,2,4-oxadiazol-3-yl]phenyl]-3-pyridinecarboxamide (**7**).* $R_f = 0.35$ (EtOAc/Hexane/MeOH 4:3:0.25). White solid, yield 66%. ^{1}H NMR (300 MHz, DMSO-d_6) δ 10.87 (s, 1H), 10.75 (s, 1H), 9.14 (s, 1H), 8.80 (d, $J = 4.8$ Hz, 1H), 8.33 (d, $J = 8.0$ Hz, 1H), 8.22 (s, 1H), 8.09–7.90 (m, 3H), 7.85 (d, $J = 6.6$ Hz, 1H), 7.66–7.29 (m, 6H), 7.19 (d, $J = 8.3$ Hz, 1H), 3.77 (s, 3H).

*4.1.1.8. N-[4-[5-[3-[[4-(acetylamino)phenylsulfonyl]amino]phenyl]-1,2,4-oxadiazol-3-yl]3-chlorophenyl]-3-pyridinecarboxamide (**8**).* $R_f = 0.40$ (EtOAc/Hexane/MeOH 4:1:0.25). White solid, yield 57%. ^{1}H NMR (300 MHz, DMSO-d_6) δ 10.85 (s, 1H), 10.60 (s, 1H), 10.29 (s, 1H), 9.15 (d, $J = 2.3$ Hz, 1H), 8.81 (dd, $J = 4.8$, 1.6 Hz, 1H), 8.34 (dt, $J = 8.2$, 1.9 Hz, 1H), 8.22 (d, $J = 1.9$ Hz, 1H), 8.05 (d, $J = 8.6$ Hz, 1H), 8.00–7.89 (m, 2H), 7.83 (d, $J = 8.0$ Hz, 1H), 7.79–7.69 (m, 4H), 7.65–7.50 (m, 2H), 7.48–7.41 (m, 1H), 2.05 (s, 3H). ^{13}C NMR (75 MHz, DMSO-d_6) δ 174.19, 169.10, 166.83, 164.75, 152.58, 148.86, 143.45, 142.34, 139.07, 139.02, 135.70, 132.50, 132.39, 132.27, 130.76, 130.06, 128.10, 124.04, 123.63, 123.21, 121.35, 120.12, 118.75, 118.70, 118.35, 24.17. HRMS exact mass of $C_{28}H_{21}ClN_6O_5S$ $(M + Na)^+$: 611.0875 amu; found: 611.0884 amu.

*4.1.1.9. N-[4-[5-[3-[[4-(acetylamino)-3-chlorophenylsulfonyl]amino] phenyl]-1,2,4-oxadiazol-3-yl]3-chlorophenyl]-3-pyridinecarboxamide (**9**).* $R_f = 0.30$ (DCM/MeOH 9.5:0.5). White solid, yield 29%. ^{1}H NMR (300 MHz, DMSO-d_6) δ 10.85 (s, 1H), 10.78 (s, 1H), 9.69 (s, 1H), 9.15 (d, $J = 2.3$ Hz, 1H), 8.80 (dd, $J = 4.8$, 1.6 Hz, 1H), 8.33 (dt, $J = 8.0$, 2.0 Hz, 1H), 8.22 (d, $J = 2.0$ Hz, 1H), 8.14–7.82 (m, 6H), 7.79–7.42 (m, 4H), 2.12 (s, 3H). ^{13}C NMR (75 MHz, DMSO-d_6) δ 174.12, 169.25, 166.83, 164.76, 152.59, 148.87, 142.36, 139.42, 138.58, 135.71, 135.06, 132.39, 132.29, 130.96, 130.06, 127.85, 126.20, 124.98, 124.90, 124.31, 124.19, 123.67, 123.62, 121.36, 120.10, 118.72, 118.65, 23.73.

*4.1.1.10. N-[4-[5-[3-[[4-(acetylamino)-3-methylphenylsulfonyl] amino]phenyl]-1,2,4-oxadiazol-3-yl]3-chlorophenyl]-3-pyridinecarboxamide (**10**).* $R_f = 0.30$ (DCM/MeOH 9.5:0.5). White solid, yield 65%. ^{1}H NMR (300 MHz, DMSO-d_6) δ 10.87 (s, 1H), 10.77 (s, 1H), 9.41 (d, $J = 4.6$ Hz, 1H), 9.14 (d, $J = 2.2$ Hz, 1H), 8.80 (d, $J = 4.1$ Hz, 1H), 8.33 (dt, $J = 8.1$, 2.0 Hz, 1H), 8.22 (d, $J = 1.9$ Hz, 1H),

8.15–7.89 (m, 4H), 7.87–7.75 (m, 1H), 7.72–7.34 (m, 5H), 2.24 (s, 3H), 2.07 (s, 3H).

*4.1.1.11. N-[4-[5-[3-[[4-(acetylamino)phenylsulfonyl]amino]phenyl]-1,2,4-oxadiazol-3-yl]phenyl]-3-pyridinecarboxamide (**11**).* $R_f = 0.35$ (EtOAc/Hexane/MeOH 4:1:0.25). White solid, yield 40%. ^{1}H NMR (300 MHz, DMSO-d_6) δ 10.76 (s, 1H), 10.64 (s, 1H), 10.32 (s, 1H), 9.14 (d, $J = 1.3$ Hz, 1H), 8.79 (dd, $J = 4.5$, 1.5 Hz, 1H), 8.37–8.28 (m, 1H), 8.12–7.99 (m, 4H), 7.90 (s, 1H), 7.83 (d, $J = 7.2$ Hz, 1H), 7.79–7.69 (m, 4H), 7.64–7.50 (m, 2H), 7.42 (d, $J = 9.3$ Hz, 1H), 2.04 (s, 3H).

*4.1.1.12. N-[4-[5-[3-[[4-(acetylamino)phenylsulfonyl]amino]phenyl]-1,2,4-oxadiazol-3-yl]2-chlorophenyl]-3-pyridinecarboxamide (**12**).* $R_f = 0.20$ (EtOAc/Hexane/MeOH 4:1:0.25). White solid, yield 53%. ^{1}H NMR (300 MHz, DMSO-d_6) δ 10.51 (s, 1H), 10.32 (s, 1H), 9.16 (dd, $J = 2.3$, 0.7 Hz, 1H), 8.81 (dd, $J = 4.8$, 1.7 Hz, 1H), 8.38–8.31 (m, 1H), 8.18 (d, $J = 1.9$ Hz, 1H), 8.10 (dd, $J = 8.4$, 1.9 Hz, 1H), 7.97–7.90 (m, 2H), 7.83 (dt, $J = 7.7$, 1.1 Hz, 1H), 7.79–7.68 (m, 4H), 7.61 (ddd, $J = 7.9$, 4.9, 0.8 Hz, 1H), 7.53 (t, $J = 8.0$ Hz, 1H), 7.46–7.40 (m, 1H), 2.03 (s, 3H). ^{13}C NMR (101 MHz, DMSO-d_6) δ 175.18, 168.99, 166.93, 164.20, 152.58, 148.82, 143.30, 139.36, 137.64, 135.60, 132.76, 130.62, 129.44, 129.39, 128.45, 127.98, 127.94, 126.26, 124.89, 124.09, 123.98, 123.63, 123.01, 118.64, 118.41, 24.07. HRMS exact mass of $C_{28}H_{21}ClN_6O_5S$ $(M + Na)^+$: 611.0875 amu; found: 611.0882 amu.

*4.1.1.13. N-[4-[5-[3-[[4-(acetylamino)phenylsulfonyl]amino]phenyl]-1,2,4-oxadiazol-3-yl]2-(trifluoromethyl)phenyl]-3-pyridinecarboxamide (**13**).* $R_f = 0.40$ (EtOAc/Hexane/MeOH 4:1:0.25). White solid, yield 55%. ^{1}H NMR (300 MHz, DMSO-d_6) δ 10.64 (d, $J = 8.7$ Hz, 2H), 10.33 (s, 1H), 9.13 (d, $J = 2.2$ Hz, 1H), 8.81 (dd, $J = 4.8$, 1.6 Hz, 1H), 8.47–8.37 (m, 2H), 8.31 (dt, $J = 8.0$, 1.8 Hz, 1H), 7.93 (t, $J = 1.8$ Hz, 1H), 7.87 (d, $J = 8.1$ Hz, 2H), 7.78–7.69 (m, 4H), 7.62 (ddd, $J = 8.1$, 4.8, 0.7 Hz, 1H), 7.55 (t, $J = 7.9$ Hz, 1H), 7.48–7.43 (m, 1H), 2.03 (s, 3H).

*4.1.1.14. N-[4-[5-[3-[[4-(acetylamino)phenylsulfonyl]amino]phenyl]-1,2,4-oxadiazol-3-yl]3-(trifluoromethyl)phenyl]-3-pyridinecarboxamide (**14**).* $R_f = 0.35$ (EtOAc/Hexane/MeOH 4:1:0.25). White solid, yield 70%. ^{1}H NMR (300 MHz, DMSO-d_6) δ 11.01 (s, 1H), 10.68 (s, 1H), 10.32 (s, 1H), 9.17 (s, 1H), 8.82 (d, $J = 4.9$ Hz, 1H), 8.49 (d, $J = 1.9$ Hz, 1H), 8.36 (dt, $J = 7.9$, 1.8 Hz, 1H), 8.29 (dd, $J = 8.5$, 2.1 Hz, 1H), 7.99 (d, $J = 8.6$ Hz, 1H), 7.90 (t, $J = 1.9$ Hz, 1H), 7.82 (dt, $J = 7.7$, 1.1 Hz, 1H), 7.78–7.69 (m, 4H), 7.66–7.59 (m, 1H), 7.54 (t, $J = 8.0$ Hz, 1H), 7.46–7.40 (m, 1H), 2.04 (s, 3H).

*4.1.1.15. N-[4-[5-[3-[[4-(acetylamino)phenylsulfonyl]amino]phenyl]-1,2,4-oxadiazol-3-yl]2-methoxyphenyl]-3-pyridinecarboxamide (**15**).* $R_f = 0.30$ (EtOAc/Hexane/MeOH 4:1:0.25). White solid, yield 42%. ^{1}H NMR (300 MHz, DMSO-d_6) δ 10.66 (s, 1H), 10.32 (s, 1H), 9.94 (s, 1H), 9.12 (d, $J = 2.0$ Hz, 1H), 8.78 (dd, $J = 4.8$, 1.6 Hz, 1H), 8.32 (dt, $J = 8.0$, 1.8 Hz, 1H), 8.10 (d, $J = 8.2$ Hz, 1H), 7.93–7.88 (m, 1H), 7.83 (d, $J = 7.9$ Hz, 1H), 7.79–7.66 (m, 6H), 7.61–7.49 (m, 2H), 7.46–7.41 (m, 1H), 3.98 (s, 3H), 2.04 (s, 3H).

*4.1.1.16. N-[4-[5-[3-[[4-(acetylamino)phenylsulfonyl]amino]phenyl]-1,2,4-oxadiazol-3-yl]3-methoxyphenyl]-3-pyridinecarboxamide (**16**).* $R_f = 0.20$ (EtOAc/MeOH 4:0.25). White solid, yield 81%. ^{1}H NMR (300 MHz, DMSO-d_6) δ 10.73 (s, 1H), 10.61 (s, 1H), 10.32 (s, 1H), 9.14 (d, $J = 2.4$ Hz, 1H), 8.79 (dd, $J = 4.8$, 1.6 Hz, 1H), 8.33 (dt, $J = 7.9$, 1.8 Hz, 1H), 7.96 (d, $J = 8.5$ Hz, 1H), 7.88 (t, $J = 1.7$ Hz, 1H), 7.84–7.69 (m, 6H), 7.68–7.55 (m, 2H), 7.52 (t, $J = 8.0$ Hz, 1H), 7.44–7.38 (m, 1H), 3.91 (s, 3H), 2.04 (s, 3H).

*4.1.1.17. N-[4-[5-[3-[[4-[(aminocarbonyl)amino]phenylsulfonyl]amino]phenyl]-1,2,4-oxadiazol-3-yl]3-chlorophenyl]-3-pyridinecarboxamide (**17**).* $R_f = 0.40$ (DCM/MeOH 9:1). White solid, yield 20%. ^{1}H NMR (300 MHz, DMSO-d_6) δ 10.88 (s, 1H), 10.60 (s, 1H), 9.15 (d, $J = 1.9$ Hz, 1H), 9.01 (s, 1H), 8.81 (dd, $J = 4.9$, 1.6 Hz, 1H), 8.34 (dt, $J = 8.0$, 1.9 Hz, 1H), 8.22 (d, $J = 2.1$ Hz, 1H), 8.06 (d, $J = 8.8$ Hz, 1H), 7.99–7.90 (m, 2H), 7.83 (d, $J = 8.0$ Hz, 1H), 7.72–7.59 (m, 3H), 7.58–7.49 (m, 3H), 7.47–7.37 (m, 1H), 6.08 (s, 2H). ^{13}C NMR (75 MHz, DMSO-d_6) δ 174.66, 167.25, 165.19, 155.91, 153.02, 149.27, 145.45, 142.75, 139.65, 136.13, 132.81, 132.72, 131.17, 130.73, 130.49, 128.51, 124.43, 124.07, 123.47, 121.76, 120.58, 120.57, 119.17, 118.54, 117.58. HRMS exact mass of $C_{27}H_{20}ClN_7O_5S$ $(M + Na)^+$: 612.0827 amu; found: 612.0845 amu.

*4.1.1.18. N-[3-chloro-4-[5-[3-[[4-[[(methylamino)carbonyl]amino]phenylsulfonyl]amino]phenyl]-1,2,4-oxadiazol-3-yl]phenyl]-3-pyridinecarboxamide (**18**).* $R_f = 0.20$ (DCM/MeOH 9.5:0.5). White solid, yield 36%. ^{1}H NMR (300 MHz, DMSO-d_6) δ 10.88 (s, 1H), 10.59 (s, 1H), 9.15 (d, $J = 1.7$ Hz, 1H), 9.02 (s, 1H), 8.81 (dd, $J = 4.9$, 1.6 Hz, 1H), 8.34 (dt, $J = 8.1$, 2.0 Hz, 1H), 8.22 (d, $J = 1.8$ Hz, 1H), 8.05 (d, $J = 8.7$ Hz, 1H), 8.00–7.89 (m, 2H), 7.82 (d, $J = 7.9$ Hz, 1H), 7.72–7.58 (m, 3H), 7.58–7.49 (m, 3H), 7.48–7.40 (m, 1H), 6.31–6.12 (m, 1H), 2.61 (d, $J = 4.6$ Hz, 3H). ^{13}C NMR (75 MHz, DMSO-d_6) δ 174.66, 167.25, 165.18, 155.66, 153.00, 149.27, 145.50, 142.76, 139.66, 136.12, 132.81, 132.70, 131.15, 130.58, 130.49, 128.52, 124.43, 124.26, 124.06, 123.45, 121.77, 120.57, 119.17, 118.56, 117.45, 26.68. HRMS exact mass of $C_{28}H_{22}ClN_7O_5S$ $(M + Na)^+$: 626.0984 amu; found: 626.0999 amu.

*4.1.1.19. N-[3-chloro-4-[5-[3-[[4-[[(ethylamino)carbonyl]amino]phenylsulfonyl]amino]phenyl]-1,2,4-oxadiazol-3-yl]phenyl]-3-pyridinecarboxamide (**19**).* $R_f = 0.20$ (EtOAc/Hexane/MeOH 4:1:0.25). White solid, yield 35%. ^{1}H NMR (300 MHz, DMSO-d_6) δ 10.87 (s, 1H), 10.58 (s, 1H), 9.14 (d, $J = 2.0$ Hz, 1H), 8.92 (s, 1H), 8.80 (dd, $J = 4.6$, 1.8 Hz, 1H), 8.33 (dt, $J = 8.1$, 2.1 Hz, 1H), 8.22 (d, $J = 2.2$ Hz, 1H), 8.10–7.87 (m, 3H), 7.82 (dt, $J = 7.5$, 1.5 Hz, 1H), 7.71–7.48 (m, 6H), 7.47–7.37 (m, 1H), 6.28 (t, $J = 5.3$ Hz, 1H), 3.07 (p, $J = 7.1$ Hz, 2H), 1.01 (t, $J = 7.1$ Hz, 3H). ^{13}C NMR (75 MHz, DMSO-d_6) δ 174.18, 166.78, 164.65, 154.48, 152.48, 148.78, 144.98, 142.26, 139.20, 135.58, 132.34, 132.16, 130.60, 130.20, 129.99, 128.02, 123.96, 123.84, 123.52, 122.96, 121.33, 120.12, 118.68, 118.17, 116.98, 33.96, 15.21. HRMS exact mass of $C_{29}H_{24}ClN_7O_5S$ $(M + Na)^+$: 640.1140 amu; found: 640.1160 amu.

*4.1.1.20. N-[3-chloro-4-[5-[3-[[4-[[(diethylamino)carbonyl]amino]phenylsulfonyl]amino]phenyl]-1,2,4-oxadiazol-3-yl]phenyl]-3-pyridinecarboxamide (**20**).* $R_f = 0.30$ (DCM/MeOH 9.5:0.5). White solid, yield 26%. ^{1}H NMR (300 MHz, DMSO-d_6) δ 10.88 (s, 1H), 10.58 (s, 1H), 9.14 (d, $J = 1.0$ Hz, 1H), 8.80 (dd, $J = 4.3$, 1.1 Hz, 1H), 8.56 (s, 1H), 8.33 (dt, $J = 7.9$, 1.9 Hz, 1H), 8.22 (d, $J = 1.8$ Hz, 1H), 8.05 (d, $J = 8.6$ Hz, 1H), 8.00–7.89 (m, 2H), 7.82 (d, $J = 7.6$ Hz, 1H), 7.74–7.57 (m, 5H), 7.54 (t, $J = 8.0$ Hz, 1H), 7.48–7.40 (m, 1H), 3.46–3.16 (m, 4H), 1.04 (t, $J = 6.9$ Hz, 6H). ^{13}C NMR (75 MHz, DMSO-d_6) δ 174.69, 167.28, 165.17, 154.26, 153.00, 149.26, 145.79, 142.76, 139.67, 136.09, 132.83, 132.68, 131.21, 131.13, 130.50, 128.01, 124.45, 124.38, 124.04, 123.49, 121.82, 120.62, 119.40, 119.20, 118.67, 41.11, 14.23.

*4.1.1.21. N-[3-chloro-4-[5-[3-[[4-[[(cyclopentylamino)carbonyl]amino]phenylsulfonyl]amino]phenyl]-1,2,4-oxadiazol-3-yl]phenyl]-3-pyridinecarboxamide (**21**).* $R_f = 0.30$ (EtOAc/Hexane/MeOH 4:1:0.25). White solid, yield 45%. ^{1}H NMR (300 MHz, DMSO-d_6) δ 10.88 (s, 1H), 10.59 (s, 1H), 9.15 (dd, $J = 2.3$, 0.9 Hz, 1H), 8.81 (dd, $J = 5.1$, 1.4 Hz, 1H), 8.73 (s, 1H), 8.34 (dt, $J = 8.1$, 2.0 Hz, 1H), 8.22 (d, $J = 2.0$ Hz, 1H), 8.05 (d, $J = 8.6$ Hz, 1H), 7.97 (dd, $J = 8.7$, 2.0 Hz, 1H), 7.91 (t, $J = 1.9$ Hz, 1H), 7.82 (d, $J = 8.3$ Hz, 1H), 7.70–7.58 (m, 3H), 7.58–7.48 (m, 3H), 7.43 (ddd, $J = 8.2$, 2.3, 1.1 Hz, 1H), 6.34 (d,

$J = 7.2$ Hz, 1H), 3.89 (p, $J = 6.6$ Hz, 1H), 1.79 (dt, $J = 12.1$, 5.9 Hz, 2H), 1.66–1.47 (m, 4H), 1.42–1.27 (m, 2H).

*4.1.1.22. N-[3-chloro-4-[5-[3-[[4-[(1-pyrrolidinylcarbonyl)amino] phenylsulfonyl] amino]phenyl]-1,2,4-oxadiazol-3-yl]phenyl]-3-pyridinecarboxamide (**22**).* $R_f = 0.25$ (EtOAc/Hexane/MeOH 4:1:0.25). White solid, yield 60%. ^{1}H NMR (300 MHz, DMSO-d_6) δ 10.84 (s, 1H), 10.54 (s, 1H), 9.15 (s, 1H), 8.80 (d, $J = 4.9$ Hz, 1H), 8.52 (s, 1H), 8.34 (d, $J = 8.0$ Hz, 1H), 8.22 (s, 1H), 8.05 (d, $J = 8.6$ Hz, 1H), 8.00–7.90 (m, 2H), 7.82 (d, $J = 7.4$ Hz, 1H), 7.72–7.66 (m, 4H), 7.64–7.50 (m, 2H), 7.48–7.41 (m, 1H), 3.34 (d, $J = 5.6$ Hz, 4H), 1.87–1.77 (m, 4H).

*4.1.1.23. N-[3-chloro-4-[5-[3-[[4-[(1-piperidinylcarbonyl)amino]phenylsulfonyl]amino] phenyl]-1,2,4-oxadiazol-3-yl]phenyl]-3-pyridinecarboxamide (**23**).* $R_f = 0.35$ (DCM/MeOH 9.5:0.5). White solid, yield 45%. ^{1}H NMR (300 MHz, DMSO-d_6) δ 10.88 (s, 1H), 10.60 (s, 1H), 9.15 (s, 1H), 8.88 (s, 1H), 8.80 (d, $J = 3.5$ Hz, 1H), 8.39–8.28 (m, 1H), 8.22 (d, $J = 1.7$ Hz, 1H), 8.05 (d, $J = 8.6$ Hz, 1H), 8.01–7.89 (m, 2H), 7.85–7.78 (m, 1H), 7.73–7.49 (m, 6H), 7.47–7.39 (m, 1H), 3.50–3.18 (m, 4H), 1.64–1.36 (m, 6H). ^{13}C NMR (75 MHz, DMSO-d_6) δ 174.65, 167.25, 165.17, 154.54, 153.01, 149.28, 145.89, 142.76, 139.66, 136.12, 132.81, 132.70, 131.14, 131.01, 130.48, 128.13, 124.42, 124.30, 124.07, 123.46, 121.77, 120.56, 119.15, 119.02, 118.58, 45.16, 25.93, 24.45.

*4.1.1.24. N-[4-[[[3-[3-[2-chloro-4-[(3-pyridinylcarbonyl)amino] phenyl]-1,2,4-oxadiazol-5-yl]phenyl]amino]sulfonyl]phenyl]-4-morpholinecarboxamide (**24**).* $R_f = 0.35$ (DCM/MeOH 9:1). White solid, yield 67%. ^{1}H NMR (300 MHz, DMSO-d_6) δ 10.84 (s, 1H), 10.56 (s, 1H), 9.15 (s, 1H), 8.94 (s, 1H), 8.80 (d, $J = 5.0$ Hz, 1H), 8.34 (d, $J = 8.4$ Hz, 1H), 8.26–8.18 (m, 1H), 8.05 (d, $J = 8.6$ Hz, 1H), 8.01–7.89 (m, 2H), 7.82 (d, $J = 8.1$ Hz, 1H), 7.75–7.48 (m, 6H), 7.48–7.41 (m, 1H), 3.64–3.52 (m, 4H), 3.47–3.37 (m, 4H).

Step g, h: To a solution of *N*-[4-[5-(3-aminophenyl)-1,2,4-oxadiazol-3-yl]-3-chlorophenyl]-3-pyridinecarboxamide (**VIc**) (0.2 g, 0.51 mmol, 1 equiv) in THF (20 ml) was added phosgene (15 wt % in toluene, 1.7 ml, 2.55 mmol, 5.0 equiv) and the reaction mixture was refluxed under N_2 for 4 h. Upon the reaction completion as indicated by TLC the solution was concentrated under reduced pressure, flushed with dry toluene. To the resulting residue was added THF (20 ml), the appropriate aniline (0.77 mmol, 1.5 equiv) and DIPEA (0.132 g, 178 μl, 1.02 mmol, 2 equiv) and the reaction mixture was refluxed under N_2 overnight. Upon completion of the reaction as indicated by TLC, the solution was concentrated, and the residue was purified by chromatography to give the desired final products (**25**–**50**).

*4.1.1.25. N-[3-chloro-4-[5-[3-[[(phenylamino)carbonyl]amino] phenyl]-1,2,4-oxadiazol-3-yl]phenyl]-3-pyridinecarboxamide (**25**).* $R_f = 0.35$ (DCM/MeOH 9.5:0.5). White solid, yield 26%. ^{1}H NMR (300 MHz, DMSO-d_6) δ 10.85 (s, 1H), 9.15 (d, $J = 2.3$ Hz, 1H), 9.08 (s, 1H), 8.80 (dd, $J = 4.9$, 1.6 Hz, 1H), 8.76 (s, 1H), 8.49 (s, 1H), 8.38–8.29 (m, 1H), 8.23 (d, $J = 2.0$ Hz, 1H), 8.09 (d, $J = 8.6$ Hz, 1H), 7.97 (dd, $J = 8.6$, 2.1 Hz, 1H), 7.79 (d, $J = 7.6$ Hz, 1H), 7.71–7.53 (m, 3H), 7.49 (d, $J = 8.1$ Hz, 2H), 7.30 (t, $J = 7.8$ Hz, 2H), 7.00 (t, $J = 7.4$ Hz, 1H).

*4.1.1.26. N-[3-chloro-4-[5-[3-[[(4-chlorophenylamino)carbonyl] amino]phenyl]-1,2,4-oxadiazol-3-yl]phenyl]-3-pyridinecarboxamide (**26**).* $R_f = 0.25$ (DCM/MeOH 9.5:0.5). White solid, yield 63%. ^{1}H NMR (300 MHz, DMSO-d_6) δ 10.85 (s, 1H), 9.14 (s, 1H), 9.12 (s, 1H), 8.91 (s, 1H), 8.80 (d, $J = 4.8$ Hz, 1H), 8.47 (s, 1H), 8.33 (d, $J = 8.0$ Hz, 1H), 8.22 (s, 1H), 8.08 (d, $J = 8.6$ Hz, 1H), 7.96 (d, $J = 8.7$ Hz, 1H), 7.80 (d, $J = 7.6$ Hz, 1H), 7.68 (d, $J = 8.3$ Hz, 1H), 7.63–7.57 (m, 2H), 7.52 (d, $J = 8.7$ Hz, 2H), 7.34 (d, $J = 8.5$ Hz, 2H).

*4.1.1.27. N-[4-[5-[3-[[[4-(aminosulfonyl)phenylamino]carbonyl] amino]phenyl]-1,2,4-oxadiazol-3-yl]-3-chlorophenyl]-3-pyridinecarboxamide (**27**).* $R_f = 0.30$ (EtOAc/Hexane/MeOH 4:1:0.25). White solid, yield 49%. ^{1}H NMR (300 MHz, DMSO-d_6) δ 10.88 (s, 1H), 9.25 (s, 1H), 9.22 (s, 1H), 9.14 (dd, $J = 2.4$, 0.9 Hz, 1H), 8.80 (dd, $J = 4.9$, 1.6 Hz, 1H), 8.51 (t, $J = 1.9$ Hz, 1H), 8.33 (dt, $J = 8.1$, 1.9 Hz, 1H), 8.23 (d, $J = 2.0$ Hz, 1H), 8.09 (d, $J = 8.6$ Hz, 1H), 7.97 (dd, $J = 8.7$, 2.1 Hz, 1H), 7.86–7.79 (m, 1H), 7.75 (d, $J = 8.7$ Hz, 2H), 7.71–7.54 (m, 5H), 7.24 (s, 2H).

*4.1.1.28. N-[3-chloro-4-[5-[3-[[(4-methylphenylamino)carbonyl] amino]phenyl]-1,2,4-oxadiazol-3-yl]phenyl]-3-pyridinecarboxamide (**28**).* $R_f = 0.30$ (DCM/MeOH 9.5:0.5). White solid, yield 15%. ^{1}H NMR (300 MHz, DMSO-d_6) δ 10.85 (s, 1H), 9.15 (s, 1H), 9.03 (s, 1H), 8.80 (d, $J = 4.8$ Hz, 1H), 8.65 (s, 1H), 8.48 (s, 1H), 8.34 (d, $J = 8.1$ Hz, 1H), 8.23 (d, $J = 2.0$ Hz, 1H), 8.08 (d, $J = 8.6$ Hz, 1H), 7.97 (d, $J = 8.7$ Hz, 1H), 7.78 (d, $J = 7.5$ Hz, 1H), 7.71–7.52 (m, 3H), 7.37 (d, $J = 8.1$ Hz, 2H), 7.11 (d, $J = 8.0$ Hz, 2H), 2.25 (s, 3H).

*4.1.1.29. N-[3-chloro-4-[5-[3-[[[3-(trifluoromethyl)phenylamino] carbonyl]amino] phenyl]-1,2,4-oxadiazol-3-yl]phenyl]-3-pyridinecarboxamide (**29**).* $R_f = 0.20$ (DCM/MeOH 9:1). White solid, yield 23%. ^{1}H NMR (300 MHz, DMSO-d_6) δ 10.85 (s, 1H), 9.15 (d, $J = 1.7$ Hz, 1H), 9.00 (s, 1H), 8.80 (dd, $J = 4.8$, 1.6 Hz, 1H), 8.56 (s, 1H), 8.47 (t, $J = 1.9$ Hz, 1H), 8.23 (d, $J = 2.1$ Hz, 1H), 8.33 (dt, $J = 8.1$, 2.0 Hz, 1H), 8.08 (d, $J = 8.6$ Hz, 1H), 7.96 (dd, $J = 8.7$, 2.1 Hz, 1H), 7.77 (dd, $J = 7.6$, 1.6 Hz, 1H), 7.71–7.50 (m, 3H), 7.39 (d, $J = 9.0$ Hz, 2H), 6.89 (d, $J = 9.0$ Hz, 2H), 3.73 (s, 3H). ^{13}C NMR (75 MHz, DMSO- d_6) δ 174.78, 166.77, 164.62, 154.69, 152.65, 152.44, 148.76, 142.21, 141.00, 135.59, 132.37, 132.33, 132.16, 130.04, 129.99, 123.61, 123.51, 122.61, 121.32, 120.90, 120.37, 120.23, 118.65, 116.82, 113.96, 55.15.

*4.1.1.30. N-[3-chloro-4-[5-[3-[[(3-methoxyphenylamino)carbonyl] amino]phenyl]-1,2,4-oxadiazol-3-yl]phenyl]-3-pyridinecarboxamide (**30**).* $R_f = 0.30$ (DCM/MeOH 9.5:0.5). White solid, yield 56%. ^{1}H NMR (300 MHz, DMSO-d_6) δ 10.85 (s, 1H), 9.15 (d, $J = 2.5$ Hz, 1H), 9.06 (s, 1H), 8.85–8.74 (m, 2H), 8.47 (t, $J = 2.0$ Hz, 1H), 8.34 (dt, $J = 8.1$, 2.0 Hz, 1H), 8.23 (d, $J = 2.0$ Hz, 1H), 8.08 (d, $J = 8.6$ Hz, 1H), 7.97 (dd, $J = 8.7$, 2.1 Hz, 1H), 7.80 (d, $J = 7.7$ Hz, 1H), 7.72–7.52 (m, 3H), 7.26–7.14 (m, 2H), 6.97 (dd, $J = 7.7$, 2.2 Hz, 1H), 6.58 (dd, $J = 8.1$, 2.5 Hz, 1H), 3.75 (s, 3H).

*4.1.1.31. N-[3-chloro-4-[5-[3-[[(4-methoxyphenylamino)carbonyl] amino]phenyl]-1,2,4-oxadiazol-3-yl]phenyl]-3-pyridinecarboxamide (**31**).* $R_f = 0.35$ (DCM/MeOH 9.8:0.2). White solid, yield 80%. ^{1}H NMR (300 MHz, DMSO-d_6) δ 10.85 (s, 1H), 9.22 (s, 1H), 9.15 (s, 2H), 8.80 (d, $J = 4.8$ Hz, 1H), 8.47 (s, 1H), 8.33 (d, $J = 8.2$ Hz, 1H), 8.23 (d, $J = 2.1$ Hz, 1H), 8.13–7.92 (m, 3H), 7.82 (d, $J = 7.6$ Hz, 1H), 7.71 (d, $J = 8.7$ Hz, 1H), 7.67–7.49 (m, 4H), 7.34 (d, $J = 7.7$ Hz, 1H). ^{13}C NMR (101 MHz, DMSO-d_6) δ 174.73, 166.80, 164.67, 152.49, 148.78, 142.25, 140.50, 140.31, 135.62, 132.33, 132.21, 130.16, 130.01, 129.90, 129.68, 129.37, 129.06, 125.53, 123.67, 123.55, 123.06, 122.82, 122.11, 121.48, 121.32, 120.22, 118.70, 118.36, 117.19, 114.39. HRMS exact mass of $C_{28}H_{18}ClF_3N_6O_3$ $(M + Na)^+$: 601.0973 amu; found: 601.0989 amu.

*4.1.1.32. N-[3-chloro-4-[5-[3-[[[4-chloro-3-(trifluoromethyl)phenylamino]carbonyl] amino]phenyl]-1,2,4-oxadiazol-3-yl]phenyl]-3-pyridinecarboxamide (**32**).* $R_f = 0.40$ (DCM/MeOH 9.8:0.2). White solid, yield 90%. ^{1}H NMR (300 MHz, DMSO-d_6) δ 10.86 (s, 1H), 9.54 (s, 1H), 9.46 (s, 1H), 9.14 (dd, $J = 2.3$, 0.9 Hz, 1H), 8.80 (dd, $J = 4.8$, 1.7 Hz, 1H), 8.46 (t, $J = 1.9$ Hz, 1H), 8.33 (dt, $J = 8.0$, 2.0 Hz, 1H), 8.22 (d, $J = 2.0$ Hz, 1H), 8.17 (s, 2H), 8.08 (d, $J = 8.6$ Hz, 1H), 7.97 (dd,

$J = 8.6$, 2.1 Hz, 1H), 7.83 (dt, $J = 7.7$, 1.3 Hz, 1H), 7.74 (dd, $J = 2.3$, 1.1 Hz, 1H), 7.67 (s, 1H), 7.65–7.55 (m, 2H).

*4.1.1.33. N-[3-chloro-4-[5-[3-[[[3,5-bis(trifluoromethyl)phenylamino]carbonyl]amino]phenyl]-1,2,4-oxadiazol-3-yl] phenyl]-3-pyridinecarboxamide (**33**).* $R_f = 0.25$ (EtOAc/Hexane/MeOH 4:4:0.25). White solid, yield 72%. ^{1}H NMR (300 MHz, DMSO-d_6) δ 10.86 (s, 1H), 9.34 (s, 2H), 9.14 (d, $J = 1.7$ Hz, 1H), 8.80 (dd, $J = 4.8$, 1.6 Hz, 1H), 8.46 (t, $J = 1.9$ Hz, 1H), 8.33 (dt, $J = 8.0$, 1.9 Hz, 1H), 8.22 (d, $J = 2.0$ Hz, 1H), 8.16–8.03 (m, 2H), 7.96 (dd, $J = 8.6$, 2.1 Hz, 1H), 7.81 (d, $J = 7.7$ Hz, 1H), 7.76–7.64 (m, 2H), 7.66–7.55 (m, 3H).

*4.1.1.34. N-[3-chloro-4-[5-[3-[[[4-methoxy-3-(trifluoromethyl)phenylamino]carbonyl] amino]phenyl]-1,2,4-oxadiazol-3-yl]phenyl]-3-pyridinecarboxamide (**34**).* $R_f = 0.20$ (EtOAc/Hexane/MeOH 4:2:0.25). White solid, yield 68%. ^{1}H NMR (300 MHz, DMSO-d_6) δ 10.84 (s, 1H), 9.18–9.11 (m, 2H), 8.88 (s, 1H), 8.80 (dd, $J = 4.8$, 1.7 Hz, 1H), 8.46 (t, $J = 2.0$ Hz, 1H), 8.33 (dt, $J = 7.9$, 2.0 Hz, 1H), 8.22 (d, $J = 2.0$ Hz, 1H), 8.08 (d, $J = 8.6$ Hz, 1H), 7.96 (dd, $J = 8.6$, 2.1 Hz, 1H), 7.85 (d, $J = 2.7$ Hz, 1H), 7.79 (dt, $J = 7.6$, 1.3 Hz, 1H), 7.70 (dd, $J = 8.7$, 1.8 Hz, 1H), 7.66–7.54 (m, 3H), 7.23 (d, $J = 9.0$ Hz, 1H), 3.86 (s, 3H). ^{13}C NMR (101 MHz, DMSO-d_6) δ 174.77, 166.79, 164.67, 152.71, 152.50, 152.15, 148.79, 142.24, 140.76, 135.60, 132.33, 132.29, 132.21, 130.11, 130.01, 124.33, 123.63, 123.54, 122.93, 121.32, 121.22, 120.23, 118.70, 117.30, 117.24, 117.07, 116.88, 113.51, 56.24. HRMS exact mass of $C_{29}H_{20}ClF_3N_6O_4$ $(M + Na)^+$: 631.1079 amu; found: 631.1089 amu.

*4.1.1.35. N-[3-chloro-4-[5-[3-[[(3-ethynylphenylamino)carbonyl] amino]phenyl]-1,2,4-oxadiazol-3-yl]phenyl]-3-pyridinecarboxamide (**35**).* $R_f = 0.30$ (EtOAc/Hexane/MeOH 4:4:0.25). White solid, yield 52%. ^{1}H NMR (300 MHz, DMSO-d_6) δ 10.87 (s, 1H), 9.21–9.11 (m, 2H), 8.91 (s, 1H), 8.80 (dd, $J = 4.9$, 1.6 Hz, 1H), 8.48 (s, 1H), 8.33 (dt, $J = 8.0$, 2.0 Hz, 1H), 8.23 (d, $J = 2.0$ Hz, 1H), 8.09 (d, $J = 8.6$ Hz, 1H), 7.96 (dd, $J = 8.7$, 2.1 Hz, 1H), 7.80 (d, $J = 8.0$ Hz, 1H), 7.74–7.52 (m, 4H), 7.50–7.40 (m, 1H), 7.31 (t, $J = 7.9$ Hz, 1H), 7.11 (dt, $J = 7.6$, 1.3 Hz, 1H), 4.19 (s, 1H). ^{13}C NMR (75 MHz, DMSO-d_6) δ 174.74, 166.79, 164.66, 152.48, 152.43, 148.77, 142.23, 140.63, 139.64, 135.58, 132.32, 132.20, 130.13, 130.00, 129.18, 125.39, 123.65, 123.53, 122.89, 122.07, 121.33, 121.30, 121.23, 120.22, 119.17, 118.70, 117.06, 83.49, 80.40.

*4.1.1.36. N-[3-chloro-4-[5-[3-[[(4-ethynylphenylamino)carbonyl] amino]phenyl]-1,2,4-oxadiazol-3-yl]phenyl]-3-pyridinecarboxamide (**36**).* $R_f = 0.25$ (EtOAc/Hexane/MeOH 4:4:0.25). White solid, yield 44%. ^{1}H NMR (300 MHz, DMSO-d_6) δ 10.87 (s, 1H), 9.21–9.11 (m, 2H), 9.02 (s, 1H), 8.80 (dd, $J = 4.8$, 1.7 Hz, 1H), 8.48 (t, $J = 1.9$ Hz, 1H), 8.33 (dt, $J = 8.0$, 2.0 Hz, 1H), 8.23 (d, $J = 2.1$ Hz, 1H), 8.09 (d, $J = 8.6$ Hz, 1H), 7.96 (dd, $J = 8.6$, 2.1 Hz, 1H), 7.80 (d, $J = 7.6$ Hz, 1H), 7.70–7.54 (m, 3H), 7.51 (d, $J = 8.7$ Hz, 2H), 7.41 (d, $J = 8.7$ Hz, 2H), 4.07 (s, 1H).

*4.1.1.37. N-[4-[5-[3-[[[4-[(aminosulfonyl)amino]phenylamino] carbonyl]amino]phenyl]-1,2,4-oxadiazol-3-yl]-3-chlorophenyl]-3-pyridinecarboxamide (**37**).* $R_f = 0.30$ (EtOAc/Hexane/MeOH 4:1:0.25). White solid, yield 21%. ^{1}H NMR (300 MHz, DMSO-d_6) δ 10.85 (s, 1H), 9.23–9.11 (m, 2H), 9.02 (s, 1H), 8.80 (dd, $J = 4.8$, 1.7 Hz, 1H), 8.64 (s, 1H), 8.52–8.44 (m, 1H), 8.34 (dt, $J = 8.0$, 2.0 Hz, 1H), 8.23 (d, $J = 2.0$ Hz, 1H), 8.08 (d, $J = 8.6$ Hz, 1H), 7.96 (dd, $J = 8.7$, 2.1 Hz, 1H), 7.78 (dt, $J = 7.5$, 1.4 Hz, 1H), 7.71–7.51 (m, 3H), 7.39 (d, $J = 8.8$ Hz, 2H), 7.12 (d, $J = 8.8$ Hz, 2H), 6.96 (s, 2H).

*4.1.1.38. N-[3-chloro-4-[5-[3-[[[3-[(methylsulfonyl)amino]phenylamino]carbonyl]amino]phenyl]-1,2,4-oxadiazol-3-yl] phenyl]-3-pyridinecarboxamide (**38**).* $R_f = 0.40$ (EtOAc/Hexane/MeOH 4:2:0.25). White solid, yield 59%. ^{1}H NMR (300 MHz, DMSO-d_6) δ 10.85 (s, 1H), 9.72 (s, 1H), 9.15 (d, $J = 1.8$ Hz, 1H), 9.03 (s, 1H), 8.88 (s, 1H), 8.80 (dd, $J = 4.8$, 1.6 Hz, 1H), 8.48 (t, $J = 1.7$ Hz, 1H), 8.34 (dt, $J = 8.1$, 2.0 Hz, 1H), 8.23 (d, $J = 2.0$ Hz, 1H), 8.08 (d, $J = 8.6$ Hz, 1H), 7.96 (dd, $J = 8.6$, 2.0 Hz, 1H), 7.80 (d, $J = 7.5$ Hz, 1H), 7.71–7.52 (m, 3H), 7.41 (d, $J = 2.1$ Hz, 1H), 7.31–7.18 (m, 2H), 6.90–6.80 (m, 1H), 3.00 (s, 3H).

*4.1.1.39. N-[3-chloro-4-[5-[3-[[[4-[(methylsulfonyl)amino]phenylamino]carbonyl] amino]phenyl]-1,2,4-oxadiazol-3-yl]phenyl]-3-pyridinecarboxamide (**39**).* $R_f = 0.35$ (EtOAc/Hexane/MeOH 4:2:0.25). White solid, yield 65%. ^{1}H NMR (300 MHz, DMSO-d_6) δ 10.84 (s, 1H), 9.46 (s, 1H), 9.15 (d, $J = 2.0$ Hz, 1H), 9.05 (s, 1H), 8.80 (dd, $J = 4.8$, 1.6 Hz, 1H), 8.75 (s, 1H), 8.48 (t, $J = 1.9$ Hz, 1H), 8.33 (dt, $J = 8.0$, 1.9 Hz, 1H), 8.23 (d, $J = 2.0$ Hz, 1H), 8.08 (d, $J = 8.6$ Hz, 1H), 7.96 (dd, $J = 8.6$, 2.0 Hz, 1H), 7.79 (d, $J = 7.6$ Hz, 1H), 7.72–7.51 (m, 3H), 7.46 (d, $J = 8.8$ Hz, 2H), 7.17 (d, $J = 8.7$ Hz, 2H), 2.93 (s, 3H). ^{13}C NMR (75 MHz, DMSO-d_6) δ 174.83, 166.84, 164.76, 153.97, 152.55, 148.86, 142.31, 140.88, 136.17, 135.71, 132.50, 132.38, 132.30, 130.22, 130.08, 123.68, 123.64, 122.79, 121.90, 121.35, 121.17, 120.25, 119.49, 118.73, 116.92, 38.84. HRMS exact mass of $C_{28}H_{22}ClN_7O_5S$ $(M + Na)^+$: 626.0984 amu; found: 626.0997 amu.

*4.1.1.40. N-[3-chloro-4-[5-[3-[[[3-chloro-4-[(methylsulfonyl)amino] phenylamino] carbonyl]amino]phenyl]-1,2,4-oxadiazol-3-yl]phenyl]-3-pyridinecarboxamide (**40**).* $R_f = 0.35$ (EtOAc/Hexane/MeOH 4:1:0.25). White solid, yield 28%. ^{1}H NMR (300 MHz, DMSO-d_6) δ 10.84 (s, 1H), 9.32 (s, 1H), 9.21–9.11 (m, 2H), 9.02 (s, 1H), 8.80 (d, $J = 3.9$ Hz, 1H), 8.47 (s, 1H), 8.33 (d, $J = 7.8$ Hz, 1H), 8.22 (d, $J = 1.9$ Hz, 1H), 8.08 (d, $J = 8.6$ Hz, 1H), 7.97 (d, $J = 8.2$ Hz, 1H), 7.87–7.76 (m, 2H), 7.73–7.52 (m, 3H), 7.42–7.28 (m, 2H), 3.00 (s, 3H). ^{13}C NMR (75 MHz, DMSO-d_6) δ 174.72, 166.79, 164.66, 152.47, 152.33, 148.77, 142.23, 140.49, 138.98, 135.58, 132.19, 132.13, 130.26, 130.14, 130.00, 129.36, 127.59, 123.66, 123.52, 122.99, 121.42, 121.32, 120.21, 118.92, 118.69, 117.71, 117.14, 40.69. HRMS exact mass of $C_{28}H_{21}Cl_2N_7O_5S$ $(M + Na)^+$: 660.0594 amu; found: 660.0608 amu.

*4.1.1.41. N-[4-[5-[3-[[[3-bromo-4-[(methylsulfonyl)amino]phenylamino]carbonyl] amino]phenyl]-1,2,4-oxadiazol-3-yl]-3-chlorophenyl]-3-pyridinecarboxamide (**41**).* $R_f = 0.35$ (EtOAc/Hexane/MeOH 4:1:0.25). White solid, yield 31%. ^{1}H NMR (300 MHz, DMSO-d_6) δ 10.88 (s, 1H), 9.32 (s, 1H), 9.24 (s, 1H), 9.18–9.04 (m, 2H), 8.80 (d, $J = 4.7$ Hz, 1H), 8.48 (s, 1H), 8.33 (d, $J = 7.9$ Hz, 1H), 8.23 (s, 1H), 8.09 (d, $J = 8.5$ Hz, 1H), 8.03–7.92 (m, 2H), 7.80 (d, $J = 7.5$ Hz, 1H), 7.73–7.52 (m, 3H), 7.43–7.30 (m, 2H), 3.01 (s, 3H).

*4.1.1.42. N-[3-chloro-4-[5-[3-[[[4-[(methylsulfonyl)amino]-3-(trifluoromethyl)phenyl-amino]carbonyl]amino]phenyl]-1,2,4-oxadiazol-3-yl]phenyl]-3-pyridinecarboxamide (**42**).* $R_f = 0.35$ (EtOAc/Hexane/MeOH 4:2:0.25). White solid, yield 18%. ^{1}H NMR (300 MHz, DMSO-d_6) δ 10.84 (s, 1H), 9.39–8.99 (m, 4H), 8.80 (dt, $J = 4.9$, 1.7 Hz, 1H), 8.47 (t, $J = 1.9$ Hz, 1H), 8.34 (ddd, $J = 8.0$, 2.3, 1.7 Hz, 1H), 8.23 (d, $J = 2.1$ Hz, 1H), 8.12–7.89 (m, 4H), 7.82 (dt, $J = 7.6$, 1.4 Hz, 1H), 7.75–7.47 (m, 4H), 3.06 (s, 3H).

*4.1.1.43. N-[3-chloro-4-[5-[3-[[[4-[(cyclopropylsulfonyl)amino]phenylamino]carbonyl] amino]phenyl]-1,2,4-oxadiazol-3-yl]phenyl]-3-pyridinecarboxamide (**43**).* $R_f = 0.20$ (EtOAc/Hexane/MeOH 4:1:0.25). White solid, yield 46%. ^{1}H NMR (300 MHz, DMSO-d_6) δ 10.87 (s, 1H), 9.50 (s, 1H), 9.11 (d, $J = 18.6$ Hz, 2H), 8.84–8.74 (m, 2H), 8.48 (s, 1H), 8.33 (d, $J = 7.5$ Hz, 1H), 8.23 (d, $J = 2.0$ Hz, 1H), 8.08 (d, $J = 8.6$ Hz, 1H), 7.96 (dd, $J = 8.7$, 2.0 Hz, 1H), 7.78 (d, $J = 7.6$ Hz, 1H), 7.70–7.50 (m, 3H), 7.45 (d, $J = 8.8$ Hz, 2H), 7.19 (d, $J = 8.6$ Hz, 2H), 2.61–2.48 (m, 1H), 0.95–0.86 (m, 4H). ^{13}C NMR (75 MHz, DMSO-d_6) δ 174.78, 166.78, 164.66, 152.48, 152.40, 148.77, 142.23, 140.82, 136.07, 135.58, 132.39, 132.32, 132.18, 130.11, 130.00, 123.63, 123.52, 122.72, 122.35, 121.32, 121.10, 120.23, 119.29, 118.68, 116.91,

29.16, 4.82. HRMS exact mass of $C_{30}H_{24}ClN_7O_5S$ $(M + Na)^+$: 652.1140 amu; found: 652.1158 amu.

*4.1.1.44. N-[4-[5-[3-[[[4-(acetylamino)phenylamino]carbonyl]amino] phenyl]-1,2,4-oxadiazol-3-yl]3-chlorophenyl]-3-pyridinecarboxamide (**44**).* $R_f = 0.35$ (EtOAc/MeOH 4:0.25). Off-white solid, yield 24%. ^1H NMR (300 MHz, DMSO-d_6) δ 10.88 (s, 1H), 9.86 (s, 1H), 9.15 (d, $J = 2.3$ Hz, 1H), 9.05 (s, 1H), 8.80 (dd, $J = 4.9$, 1.7 Hz, 1H), 8.69 (s, 1H), 8.49 (t, $J = 1.9$ Hz, 1H), 8.33 (dt, $J = 8.0$, 2.0 Hz, 1H), 8.23 (d, $J = 2.0$ Hz, 1H), 8.09 (d, $J = 8.6$ Hz, 1H), 7.96 (dd, $J = 8.7$, 2.1 Hz, 1H), 7.78 (dt, $J = 7.4$, 1.5 Hz, 1H), 7.68–7.53 (m, 3H), 7.50 (d, $J = 9.1$ Hz, 2H), 7.40 (d, $J = 9.0$ Hz, 2H), 2.02 (s, 3H).

*4.1.1.45. N-[4-[5-[3-[[[4-(acetylamino)-3-chlorophenylamino] carbonyl]amino]phenyl]-1,2,4-oxadiazol-3-yl]3-chlorophenyl]-3-pyridinecarboxamide (**45**).* $R_f = 0.25$ (EtOAc/Hexane/MeOH 4:1:0.25). White solid, yield 44%. ^1H NMR (300 MHz, DMSO-d_6) δ 10.88 (s, 1H), 9.47 (s, 1H), 9.21–9.11 (m, 2H), 8.97 (s, 1H), 8.80 (dd, $J = 4.8$, 1.7 Hz, 1H), 8.48 (t, $J = 2.0$ Hz, 1H), 8.34 (dt, $J = 8.0$, 2.0 Hz, 1H), 8.23 (d, $J = 2.0$ Hz, 1H), 8.09 (d, $J = 8.6$ Hz, 1H), 7.97 (dd, $J = 8.7$, 2.1 Hz, 1H), 7.85–7.76 (m, 2H), 7.72–7.48 (m, 4H), 7.28 (dd, $J = 8.7$, 2.3 Hz, 1H), 2.06 (s, 3H).

*4.1.1.46. N-[4-[5-[3-[[[4-(acetylamino)-3-bromophenylamino] carbonyl]amino]phenyl]-1,2,4-oxadiazol-3-yl]3-chlorophenyl]-3-pyridinecarboxamide (**46**).* $R_f = 0.25$ (EtOAc/Hexane/MeOH 4:1:0.25). White solid, yield 62%. ^1H NMR (300 MHz, DMSO-d_6) δ 10.88 (s, 1H), 9.43 (s, 1H), 9.22–9.11 (m, 2H), 8.97 (s, 1H), 8.80 (dd, $J = 4.7$, 1.1 Hz, 1H), 8.48 (s, 1H), 8.33 (dt, $J = 7.9$, 1.9 Hz, 1H), 8.23 (d, $J = 2.0$ Hz, 1H), 8.09 (d, $J = 8.6$ Hz, 1H), 8.02–7.92 (m, 2H), 7.80 (d, $J = 7.5$ Hz, 1H), 7.72–7.52 (m, 3H), 7.43 (d, $J = 8.7$ Hz, 1H), 7.33 (d, $J = 9.1$ Hz, 1H), 2.05 (s, 3H).

*4.1.1.47. N-[3-chloro-4-[5-[3-[[[4-[(cyclopentylcarbonyl)amino]-3-(trifluoromethyl) phenylamino]carbonyl]amino]phenyl]-1,2,4-oxadiazol-3-yl]phenyl]-3-pyridine-carboxamide (**47**).* $R_f = 0.30$ (EtOAc/Hexane/MeOH 4:1:0.25). Light-pink solid, yield 49%. ^1H NMR (300 MHz, DMSO-d_6) δ 10.86 (s, 1H), 9.39 (s, 1H), 9.26–9.11 (m, 3H), 8.80 (d, $J = 3.7$ Hz, 1H), 8.47 (d, $J = 2.5$ Hz, 1H), 8.33 (d, $J = 7.3$ Hz, 1H), 8.22 (d, $J = 2.2$ Hz, 1H), 8.08 (d, $J = 8.6$ Hz, 1H), 8.03–7.91 (m, 2H), 7.80 (d, $J = 7.6$ Hz, 1H), 7.70 (d, $J = 8.2$ Hz, 1H), 7.66–7.52 (m, 3H), 7.33 (d, $J = 8.7$ Hz, 1H), 2.83 (p, $J = 7.9$ Hz, 1H), 1.93–1.47 (m, 8H). ^{13}C NMR (75 MHz, DMSO-d_6) δ 175.72, 175.20, 167.28, 165.13, 152.98, 152.96, 149.27, 142.71, 141.00, 138.42, 136.06, 132.82, 132.66, 131.81, 130.60, 130.48, 129.91, 129.88, 125.75, 124.15, 124.00, 123.54, 122.80, 122.13, 121.93, 121.81, 120.71, 119.16, 117.70, 44.71, 30.25, 26.08. HRMS exact mass of $C_{34}H_{27}ClF_3N_7O_4$ $(M + Na)^+$: 712.1657 amu; found: 712.1669 amu.

*4.1.1.48. N-[3-chloro-4-[5-[3-[[[4-[(cyclopropylcarbonyl)amino]-3-(trifluoromethyl) phenylamino]carbonyl]amino]phenyl]-1,2,4-oxadiazol-3-yl]phenyl]-3-pyridine-carboxamide (**48**).* $R_f = 0.30$ (EtOAc/MeOH 4:0.25). Off-white solid, yield 65%. ^1H NMR (300 MHz, DMSO-d_6) δ 10.86 (s, 1H), 9.68 (s, 1H), 9.23 (s, 1H), 9.19–9.09 (m, 2H), 8.79 (dd, $J = 4.8$, 1.6 Hz, 1H), 8.47 (t, $J = 1.8$ Hz, 1H), 8.32 (dt, $J = 7.9$, 1.8 Hz, 1H), 8.22 (d, $J = 2.0$ Hz, 1H), 8.08 (d, $J = 8.6$ Hz, 1H), 8.02–7.92 (m, 2H), 7.80 (dt, $J = 7.6$, 1.0 Hz, 1H), 7.69 (ddd, $J = 8.3$, 2.0, 0.9 Hz, 1H), 7.64–7.52 (m, 3H), 7.35 (d, $J = 8.9$ Hz, 1H), 1.93–1.81 (m, 1H), 0.76 (d, $J = 4.4$ Hz, 4H). ^{13}C NMR (75 MHz, DMSO-d_6) δ 174.79, 172.87, 166.85, 164.76, 152.57, 148.85, 142.31, 140.58, 137.94, 135.70, 132.38, 132.32, 131.29, 130.25, 130.07, 129.31, 125.32, 123.69, 123.64, 123.14, 122.40, 121.70, 121.53, 121.35, 120.25, 118.75, 117.24, 115.57, 115.49, 13.71, 7.04. HRMS exact mass of $C_{32}H_{23}ClF_3N_7O_4$ $(M + Na)^+$: 684.1344 amu; found: 684.1355 amu.

*4.1.1.49. N-[3-chloro-4-[5-[3-[[[4-[(2-thienylcarbonyl)amino]-3-(trifluoromethyl) phenylamino]carbonyl]amino]phenyl]-1,2,4-oxadiazol-3-yl]phenyl]-3-pyridine-carboxamide (**49**).* $R_f = 0.30$ (EtOAc/Hexane/MeOH 4:1:0.25). Light-pink solid, yield 44%. ^1H NMR (300 MHz, DMSO-d_6) δ 10.87 (s, 1H), 10.07 (s, 1H), 9.26 (d, $J = 12.8$ Hz, 2H), 9.15 (d, $J = 2.3$ Hz, 1H), 8.80 (d, $J = 2.9$ Hz, 1H), 8.49 (s, 1H), 8.33 (d, $J = 8.1$ Hz, 1H), 8.23 (d, $J = 2.2$ Hz, 1H), 8.14–8.04 (m, 2H), 8.02–7.91 (m, 2H), 7.90–7.77 (m, 2H), 7.77–7.53 (m, 4H), 7.44 (d, $J = 8.6$ Hz, 1H), 7.23 (t, $J = 4.2$ Hz, 1H). ^{13}C NMR (75 MHz, DMSO-d_6) δ 175.22, 167.30, 165.15, 161.52, 153.01, 149.27, 142.73, 140.98, 139.59, 139.26, 136.08, 132.83, 132.69, 132.53, 132.14, 130.65, 130.49, 129.76, 129.12, 128.54, 127.55, 127.16, 125.72, 124.16, 124.02, 123.61, 122.92, 122.09, 122.01, 121.82, 120.71, 119.19, 117.76.

*4.1.1.50. N-[4-[5-[3-[[[4-[(aminocarbonyl)amino]-3-(trifluoromethyl)phenylamino] carbonyl]amino]phenyl]-1,2,4-oxadiazol-3-yl]3-chlorophenyl]-3-pyridine-carboxamide (**50**).* $R_f = 0.30$ (EtOAc/MeOH 4:0.25). White solid, yield 26%. ^1H NMR (300 MHz, DMSO-d_6) δ 10.86 (s, 1H), 9.23–9.07 (m, 2H), 9.01 (s, 1H), 8.79 (dd, $J = 4.8$, 1.7 Hz, 1H), 8.46 (t, $J = 2.0$ Hz, 1H), 8.33 (dt, $J = 8.0$, 1.9 Hz, 1H), 8.22 (d, $J = 2.0$ Hz, 1H), 8.08 (d, $J = 8.6$ Hz, 1H), 8.01–7.91 (m, 2H), 7.84–7.47 (m, 7H), 6.24 (s, 2H). ^{13}C NMR (75 MHz, DMSO-d_6) δ 174.80, 166.84, 164.75, 156.19, 152.62, 152.58, 148.86, 142.31, 140.70, 135.70, 135.12, 132.38, 132.31, 131.31, 130.22, 130.07, 127.30, 125.73, 123.69, 123.63, 123.03, 122.69, 122.11, 121.35, 120.74, 120.35, 120.25, 118.74, 117.12.

4.2. Biological activity

4.2.1. Cell lines, cell culture, reagents, and antibodies

The MDA-MB-231 breast cancer, A549 (wild-type) and H1975 (L858R/T790M) lung cancer cell lines were purchased from the American Type Culture Collection (ATCC) (Manassas, VA). PC9 (exon 19 deletion, Del19) CL68 (Del19/T790M), and CL97 (G719A/T790M) cell lines were kindly provided by Professor Pan-Chyr Yang (Institute of Biomedical Science, Academia Sinica, Taiwan) [35], among which CL68 and CL97 cell lines were established from patients who provided informed consent and with the approval of the institutional review board (National Taiwan University Hospital Research Ethics Committee). MDA-MB-231 and A549 cells were cultured in DMEM medium (Life Technologies; Grand Island, NY), and H1975, PC9, CL68, and CL97 cells were maintained in RPMI 1640 medium (Life Technologies), both of which were supplemented with 10% fetal bovine serum (FBS), 100 U/ml penicillin, and 100 μg/ml streptomycin (Life Technologies). Cells were incubated at 37 °C in a humidified incubator containing 5% CO_2. Chemical agents and antibodies used in this study were purchased from the following sources. Chemical agents: gefitinib, erlotinib, afatinib and omisertinib were purchased from Cayman Chemical (Ann Arbor, MI); protease inhibitor, phosphatase inhibitor, MTT [3-(4,5-dimethylthiazol-2-yl)-2,5-diphenyl-*2H*-tetrazolium bromide] (Sigma-Aldrich; St. Louis, MO); BCA Protein Assay kit (Thermo Fisher Scientific; Waltham, MA); Western Lighting Chemiluminescence Plus-ECL (PerkinElmer; Waltham, MA). Antibodies: EGFR, GAPDH, HRP-conjugated anti-mouse, goat and rabbit secondary antibodies (Santa Cruz Biotechnology; Santa Cruz, CA); c-Met, S473-Akt, Akt (Cell Signaling; Beverly, MA); Alexa Fluor 555- and 488-conjugated goat anti-rabbit and anti-mouse IgG (Life Technologies).

4.2.2. MTT cell viability assays

To determine the drug effects on cell viability, cells were seeded onto 96-well plates at a density of 5000 cells per well in the presence of 10% FBS. After overnight incubation, cells were exposed to test agents or DMSO in the presence of 5% FBS for 48 h. After

treatment, cells were incubated with MTT for an additional 1 h. The medium was then removed from each well and replaced with DMSO to dissolve the reduced MTT dye for subsequent colorimetric measurement of absorbance at 570 nm. Cell viabilities are expressed as percentages of viable cells relative to the corresponding vehicle-treated control group.

4.2.3. Cell lysis and immunoblotting

Drug-treated cells were collected by scrapping and then lysed in SDS lysis buffer (1% SDS, 50 mM Tris-HCl pH8.0, 10 mM EDTA) containing a commercial cocktail of protease inhibitors and phosphatase inhibitors. Lysates were sonicated and then centrifuged at 13,000 rpm for 10 min. Protein concentrations in the supernatants were determined by the BCA Protein Assay kit, and equal amounts of proteins were resolved via SDS-PAGE and transferred to a nitrocellulose membrane (GE Healthcare Life Sciences, Pittsburgh, PA). The membrane was washed twice with Tris-buffered saline containing 0.1% Tween-20 (TBST), blocked with TBST containing 5% non-fat milk for 30 min, and then incubated with primary antibody (1:1000 dilution) in TBST at 4 °C overnight. After washing with TBST, the membrane was incubated with goat anti-rabbit or anti-mouse IgG–HRP conjugates (1:5000 dilution) for 1 h at room temperature. The immunoblots were visualized by the Western Lighting Chemiluminescence Reagent Plus-ECL.

4.2.4. RNA extraction and RT-PCR analysis

Total RNA was isolated from cells using TRIzol reagent (Thermo Fisher Scientific) according to the manufacturer's protocol. One μg RNA from each sample was reverse-transcribed into cDNA using the iScript™ cDNA Synthesis Kit (Bio-Rad; Hercules, CA), and the cDNA were separated by electrophoresis. PCR products were resolved by electrophoresis in 2% agarose gels and visualized by ethidium bromide staining. The sequences of primers used for RT-PCR were as follow: EGFR, forward primer: 5′- GGC ACT TTT GAA GAT CAT TTT CTC-3′; reverse primer: 5′- CTG TGT TGA GGG CAA TGA G -3′ (144 bp). c-Met, forward primer: 5′- CAT GCC GAC AAG TGC AGT A -3′; reverse primer: 5′- TCT TGC CAT CAT TGT CCA AC-3′ (252 bp). GAPDH, forward primer: 5′- AAG CCC ATC ACC ATC TTC CAG-3′; reverse primer: 5′- AGG GGC CAT CCA CAG TCT TCT -3′ (361 bp).

4.2.5. Flow cytometry

Cells were placed into 6-cm culture dishes at 3×10^5/well in respective media overnight. After attachment, cells were treated with compound **48** at indicated concentrations for 24 h and 48 h, and the pellets were collected and fixed in 70% ethanol. Treated cell pellets were stained with 40 μg/ml of propidium iodide (PI) (Sigma-Aldrich) containing 20 μg/ml of RNase A (Sigma-Aldrich) on ice in the dark for 30 min before analysis. Cells were sorted and analyzed using a FACSCalibur flow cytometry (BD Biosciences; Franklin Lakes, NJ).

4.2.6. In vivo nude mice xenograft tumor model

Female Balb/c nude mice (Athymic Nude-Foxn1^{nu}; 5 weeks of age; National Animal Research Laboratory, Taipei, Taiwan) were group-housed under constant photoperiod (12-h light/12-h dark) with *ad libitum* access to sterilized food and water. All experimental procedures were done according to protocols approved by the Academia Sinica Animal Care Ethics Commission. To assess the effect of **48** on TKI resistant tumor growth, *in vivo,* H1975 cells were harvested and subcutaneously injected in the right flank of mice (10^6 cells/0.1 ml per mouse). When tumor volumes reached approximately 50 mm^3, mice were randomized to different groups (n = 8/each group). For the single agent *in vivo* efficacy study, mice were treated once daily for 20 days by oral gavage with vehicle solution (10% DMSO/0.1% Tween 80/0.5% methylcellulose [v/v] in sterile water), or **48** at 50 mg/kg and 150 mg/kg. For the *in vivo* efficacy of combining **48** with gefitinib, mice were divided into the following four groups, and treated once daily for 20 days by oral gavage as follows. (A) Control group, the aforementioned vehicle, (B) gefitinib at 50 mg/kg, (C) **48** at 50 mg/kg, and (D) **48** plus gefitinib, 50 mg/kg each. Tumors were measured with calipers and the volumes were calculated using V = (width^2 x length) x 0.52. Body weight and tumor volumes were monitored twice a week. At the end of the study, mice were sacrificed by CO_2 asphyxiation and tumor samples were analyzed by Western blot.

4.2.7. Statistical analysis

In vitro experiments were performed at least three times and data are presented as means ± SD. Group means were compared using one-way ANOVA followed by Student's t tests. For the *in vivo* experiments, differences in tumor volume were analyzed by Student's t-test. Differences were considered significant at $P < 0.05$.

Author contributions

C.S.C. and K.A.M. conceived the study, and designed experiments; E.M.E.D was responsible for the synthesis of all compounds; C.S.F. performed biochemical experiments; C.S.C, C.S.F and E.M.E.D wrote the manuscript and all authors revised it.

Conflicts of interest

The authors declare no competing financial interest.

Acknowledgment

PC9, CL68 and CL97 lung cancer cells were kindly provided by Dr. Pan-Chyr Yang (Institute of Biomedical Science, Academia Sinica, Taiwan). The authors are grateful to Fatma Almenier for her kind help. This work was supported, in part, by the intramural grants CMU-1065918B, 1075955A, and 1085955A from China Medical University (C.S.C).

Appendix A. Supplementary data

Supplementary data to this article can be found online at https://doi.org/10.1016/j.ejmech.2019.111607.

References

[1] A. Sudhakar, History of cancer, ancient and modern treatment methods, J. Cancer Sci. Ther. 01 (2009) i–iv.
[2] C.M. Croce, Oncogenes and cancer, N. Engl. J. Med. 358 (2008) 502–511.
[3] D. Ray, K.C. Cuneo, A. Rehemtulla, T.S. Lawrence, M.K. Nyati, Inducing oncoprotein degradation to improve targeted cancer therapy, Neoplasia 17 (2015) 697–703.
[4] H. Lei, W. Wang, Y. Wu, Targeting oncoproteins for degradation by small molecules in myeloid leukemia, Leuk. Lymphoma 59 (2018) 2297–2304.
[5] K. Raina, C.M. Crews, Chemical inducers of targeted protein degradation, J. Biol. Chem. 285 (2010) 11057–11060.
[6] D.P. Bondeson, C.M. Crews, Targeted protein degradation by small molecules, Annu. Rev. Pharmacol. Toxicol. 57 (2017) 107–123.
[7] M.A. Olayioye, R.M. Neve, H.A. Lane, N.E. Hynes, NEW EMBO MEMBERS' REVIEW: the ErbB signaling network: receptor heterodimerization in development and cancer, EMBO J. 19 (2000) 3159–3167.
[8] N. Normanno, C. Bianco, A. De Luca, M.R. Maiello, D.S. Salomon, Target-based agents against ErbB receptors and their ligands: a novel approach to cancer treatment, Endocr. Relat. Cancer 10 (2003) 1–21.
[9] J.A. Engelman, et al., MET amplification leads to gefitinib resistance in lung cancer by activating ERBB3 signaling, Science 316 (2007) 1039–1043.
[10] R. Barouch-Bentov, K. Sauer, Mechanisms of drug resistance in kinases, Expert Opin. Investig. Drugs 20 (2011) 153–208.
[11] A. Ahsan, Mechanisms of resistance to egfr tyrosine kinase inhibitors and therapeutic approaches: an update, in: A. Ahmad, S. Gadgeel (Eds.), Lung Cancer and Personalized Medicine. Advances in Experimental Medicine and Biology, vol. 893, Springer, Cham, 2016.

[12] P. Maione, et al., Irreversible EGFR inhibitors in the treatment of advanced NSCLC, Curr. Pharmaceut. Des. 20 (2014) 3894–3900.
[13] A. Murtuza, et al., Novel third-generation EGFR tyrosine kinase inhibitors and strategies to overcome therapeutic resistance in lung cancer, Cancer Res. 79 (2019) 689–698.
[14] H. Hasegawa, et al., Efficacy of afatinib or osimertinib plus cetuximab combination therapy for non-small-cell lung cancer with EGFR exon 20 insertion mutations, Lung Cancer 127 (2019) 146–152.
[15] K. Uchibori, et al., Brigatinib combined with anti-EGFR antibody overcomes osimertinib resistance in EGFR-mutated non-small-cell lung cancer, Nat. Commun. 8 (2017) 14768.
[16] Q. Wang, S. Yang, K. Wang, S.-Y. Sun, MET inhibitors for targeted therapy of EGFR TKI-resistant lung cancer, J. Hematol. Oncol. 12 (2019) 63.
[17] Z. Tang, et al., Dual MET-EGFR combinatorial inhibition against T790M-EGFR-mediated erlotinib-resistant lung cancer, Br. J. Canc. 99 (2008) 911–922.
[18] A. Kirisits, D. Pils, M. Krainer, Epidermal growth factor receptor degradation: an alternative view of oncogenic pathways☆, Int. J. Biochem. Cell Biol. 39 (2007) 2173–2182.
[19] C.-H. Jeong, H.B. Park, W.J. Jang, S.H. Jung, Y.H. Seo, Discovery of hybrid Hsp90 inhibitors and their anti-neoplastic effects against gefitinib-resistant non-small cell lung cancer (NSCLC), Bioorg. Med. Chem. Lett. 24 (2014) 224–227.
[20] Y. Wang, J.B. Trepel, L.M. Neckers, G. Giaccone, STA-9090, a small-molecule Hsp90 inhibitor for the potential treatment of cancer, Curr. Opin. Investig. Drugs 11 (2010) 1466–1476.
[21] D.-W. Wu, T.-C. Chen, H.-S. Huang, H. Lee, TC-N19, a novel dual inhibitor of EGFR and cMET, efficiently overcomes EGFR-TKI resistance in non-small-cell lung cancer cells, Cell Death Dis. 7 (2016) e2290–e2290.
[22] H.S. Huang, H. Li, Composition containing thiochrome [2,3-c] quinolin-12-one derivative for treating non-small cell lung cancer, Jpn. Tokyo Koho 17 (2018).
[23] Y. Oh, S. Park, Y. Seo, The targeted inhibition of Hsp90 by a synthetic small molecule, DPide offers an effective treatment strategy against TNBCs, Oncol. Rep. 39 (2007) 2173–2182, https://doi.org/10.3892/or.2018.6250.
[24] S.-L. Lee, et al., Identification and characterization of a novel integrin-linked kinase inhibitor, J. Med. Chem. 54 (2011) 6364–6374.
[25] K.-Y. Huang, et al., Small molecule T315 promotes casitas B-lineage lymphoma–dependent degradation of epidermal growth factor receptor via Y1045 autophosphorylation, Am. J. Respir. Crit. Care Med. 193 (2016) 753–766.
[26] J. Hughes, S. Rees, S. Kalindjian, K. Philpott, Principles of early drug discovery, Br. J. Pharmacol. 162 (2011) 1239–1249.
[27] T.J. Lynch, et al., Activating mutations in the epidermal growth factor receptor underlying responsiveness of non–small-cell lung cancer to gefitinib, N. Engl. J. Med. 350 (2004) 2129–2139.
[28] S. Kobayashi, et al., *EGFR* mutation and resistance of non–small-cell lung cancer to gefitinib, N. Engl. J. Med. 352 (2005) 786–792.
[29] M. Roengvoraphoj, G.J. Tsongalis, K.H. Dragnev, J.R. Rigas, Epidermal growth factor receptor tyrosine kinase inhibitors as initial therapy for non-small cell lung cancer: focus on epidermal growth factor receptor mutation testing and mutation-positive patients, Cancer Treat. Rev. 39 (2013) 839–850.
[30] C.-S. Kang, et al., Suppression of EGFR expression by antisense or small interference RNA inhibits U251 glioma cell growth in vitro and in vivo, Cancer Gene Ther. 13 (2006) 530–538.
[31] W. Zhou, et al., Novel mutant-selective EGFR kinase inhibitors against EGFR T790M, Nature 462 (2009) 1070–1074.
[32] C.-H. Yun, et al., The T790M mutation in EGFR kinase causes drug resistance by increasing the affinity for ATP, Proc. Natl. Acad. Sci. U. S. A 105 (2008) 2070–2075.
[33] W. Pao, et al., Acquired resistance of lung adenocarcinomas to gefitinib or erlotinib is associated with a second mutation in the EGFR kinase domain, PLoS Med. 2 (2005) e73.
[34] K.S. Thress, et al., Acquired EGFR C797S mutation mediates resistance to AZD9291 in non–small cell lung cancer harboring EGFR T790M, Nat. Med. 21 (2015) 560–562.
[35] H.-Y. Yen, et al., Effect of sialylation on EGFR phosphorylation and resistance to tyrosine kinase inhibition, Proc. Natl. Acad. Sci. U. S. A 112 (2015) 6955–6960.